TROPOS
Leibniz Institute for
Tropospheric Research

Leibniz-Institut für Troposphärenforschung Permoserstraße 15 D-04318 Leipzig

Prof. Hartmut Herrmann
Head of TROPOS Atmospheric
Chemistry Department
herrmann@tropos.de
phon: +49 341 2717 7024
fax: +49 341 2717 99 7023
Permoserstraße 15
04318 Leipzig
27.08.2020

The Editor
Atmospheric Chemistry and Physics

Submission of revision for the Atmospheric Chemistry and Physics "Minor Revision" manuscript 'Role of the dew water on the ground surface in HONO distribution: a case measurement in Melpitz' (MS No.: acp-2019-1088) by by Yangang Ren, Bastian Stieger, Gerald Spindler, Benoit Grosselin, Abdelwahid Mellouki, Thomas Tuch, Alfred Wiedensohler and Hartmut Herrmann

Dear Editor,

Please find attached here our response to the reviewer comments for the manuscript mentioned above together with its revised versions of the manuscript and supplement. We would like to thank both the editor and reviewer for all of their valuable and insightful comments to improve the manuscript. We have carefully considered all the reviewer comments and revised the manuscript accordingly. Below, we provide responses to the comments in blue, with changes made in green in the manuscript.

Sincerely yours,

Prof. Dr. H. Herrmann
Professor of Atmospheric Chemistry
Head of TROPOS Atmospheric Chemistry Department

The authors gratefully thank the editor for the comments and suggestions. We have revised our manuscript according to the reviewer's suggestions and comments. **All the changes and responses to the reviewers' comments are listed below point-by-point in blue according to a new line numbering in the revised manuscript. The major changes are highlighted with green in the revised manuscript.**

Editor Decision: Publish subject to minor revisions (review by editor) (17 Aug 2020) by Hang Su

Comments to the Author:

Dear authors,

Please find enclosed some additional comments from the reviewer. There are still some technical issues to be answered/clarified. Please revise the manuscript accordingly.

For the reviewer's concern about S/V calculations, I'd suggest you to include complementary information such as PM2.5 concentration and aerosol number concentration at both your sites and the Beijing site that you were referring to. A comparison of these numbers will help to justify your calculations.

Response: We thank the editor for the suggestion. We should mention that the reported S_a values of (5.1-9.9) $\times10^{-4}$ m^2 m^{-3} and RH corrected value of (0.6-1.9) $\times10^{-3}$ m^2 m^{-3} correspond to the night-time period 18:00-22:00 (UTC) since only nighttime data was used to calculate the HONO formation through heterogeneous conversion of NO_2. As shown in Figure R1 (we also add it in SI as Figure S5b), the S_a values ranged from 4.2×10^{-5} to 9.9×10^{-4} m^2 m^{-3} for whole day period during our field measurement period of April 19th -29th 2018, this value is one magnitude lower than S_a value of 0.2-3.4$\times10^{-3}$ m^2 m^{-3} in Beijing (Liu et al., 2014;Wang et al., 2016). However, due to the high RH (RH ~100% during nighttime in Figure R1), the S_a values would be strongly enhanced by the RH correction (Figure R1) to be (0.5-1.9)$\times10^{-3}$ m^2 m^{-3}.

In addition, we also plot 30 mins averaged $PM_{2.5}$ concentration in Figure R2, which ranged from 2 μg m^{-3} to 36 μg m^{-3} but could increase to ~257 μg m^{-3} for some nighttime period (e.g. 21:00-22:00 UTC April 19th 2018), according to our calculated S_a values of (0.4-9.9)$\times10^{-4}$ m^2 m^{-3}. Exactly, Wang et al. (2016) reported S_a value of 1.3×10^{-3} m^2 m^{-3} and 3.4×10^{-3} m^2 m^{-3}, respectively, for a clean period ($PM_{2.5}$ 0.2-107 μg m^{-3}) and a polluted period ($PM_{2.5}$ 74-192 μg m^{-3}) in the campaign Beijing 2015. Cai et al. (2017) reported a S_a value of 2×10^{-4} m^2 m^{-3} according to $PM_{2.5}$ mass concentrations of 30 μg m^{-3} during Beijing 2016. Hence, our calculated S_a value of (0.4-9.9)$\times10^{-4}$ m^2 m^{-3} is reasonable.

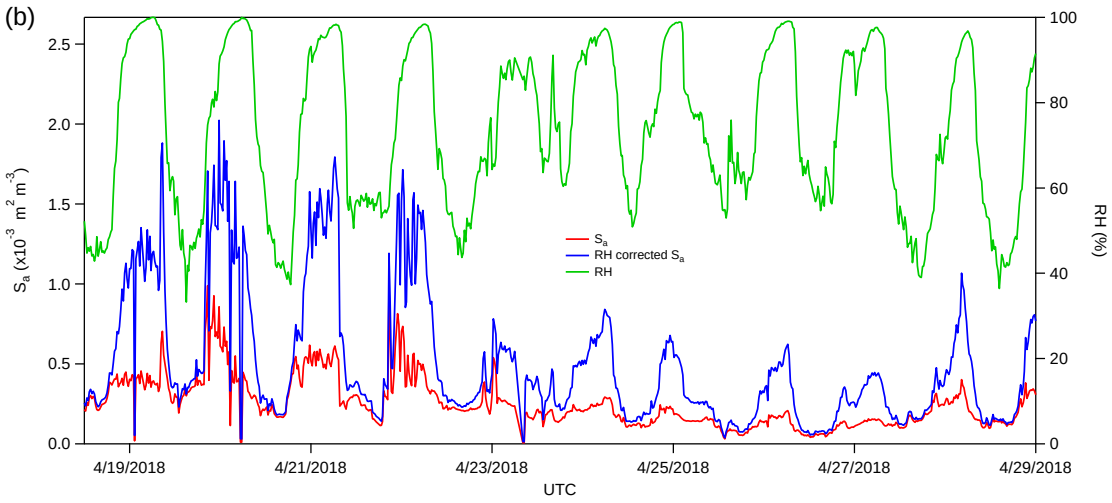

Figure R1. The particle surface density S_a and RH corrected S_a value calculated from the particle size distribution for our field measurement period of April 19th-29th 2018.

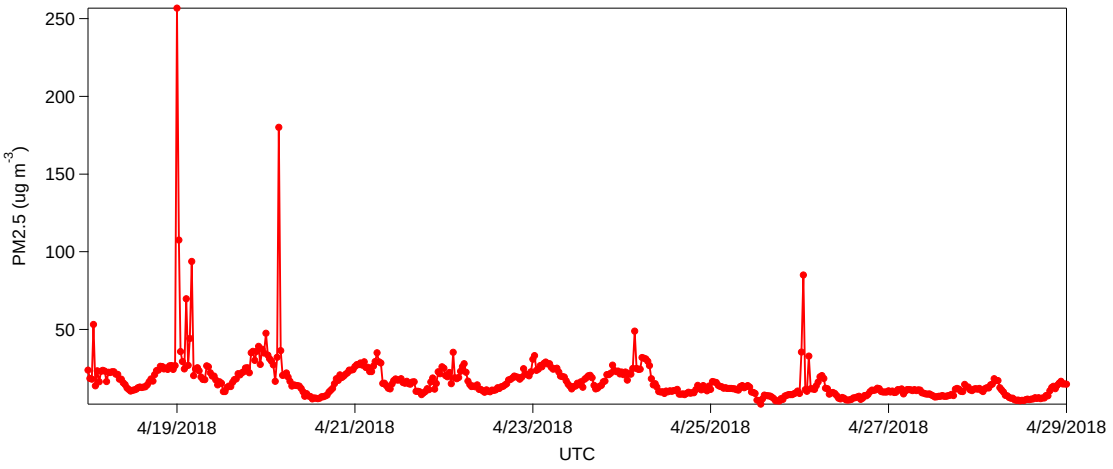

Figure R2. Time series of $PM_{2.5}$ for our field measurement period of April 19th-29th 2018.

Another question is about the calculation of dew volume. You seem to consider the dew formation as a kinetic-limited process and thus assume a dew volume proportional to the condensable surface area. Is this well-established/accepted? Otherwise, if dew formation is controlled by the thermodynamic equilibrium, it will not depend on the surface areas, but rather the difference between atmospheric temperature and the dew point temperature.

Response: As generally well known, dew occurs when the surface temperature is lower than or equal to the dew-point temperature, and water vapor from the air in contact with the cold surface condenses to form dew (Vuollekoski et al., 2015;Agam and Berliner, 2006). Exactly, the actual amount of dew in a specific place is strongly dependent on temperature and wetting properties of the surface. These two parameters control the nucleation rate and the latter has in addition major consequences on the form and growth of the droplet pattern. (Nilsson et al., 1994;Beysens, 1995). Beysens (1995) also mention that the wetting properties of a surface

can be easily modified by surface treatments. Recently, the study of Kotzen (2015) clearly indicated that main ways to maximize dew formation and collection is to increase the surface area of the collector and facilitating maximum radiative cooling to the open sky on the surface. Concerning on this work, we used one 1.5 m^2 glass sampler. Firstly, this artificial material could be less effective in collecting dew than grasses leaves since nature also tells us that multiple surfaces as well as smaller surfaces may be more effective in collecting dew. (Kotzen, 2015). Secondly this flat 1.5 m^2 glass sampler could not represent the realistic surface area of grasses leaves on the ground, where the surface area of the grasses leaves really control the dew volume around Melpitz station. Wentworth et al. (2016) and Groh et al. (2018) indicated that the dew yield of artificial devices used to collect dew would differ from that of dynamic and heterogeneous natural land surface coverages. Hence, in this work, an enhanced factor was calculated as 2 ×LAI to take the areas on both sides of the leaves and the vegetation-covered areas on the ground into account. In Wohlfahrt et al. (2001), the LAI for meadows with different grass heights are given. Regarding on the possibly different grass height during the HONO field measurement and dew measurements in April 2018 and May 2019, respectively, we would use a range of 1-6 for LAI in this version.

References

Agam, N., and Berliner, P. R.: Dew formation and water vapor adsorption in semi-arid environments—A review, Journal of Arid Environments, 65, 572-590, https://doi.org/10.1016/j.jaridenv.2005.09.004, 2006.

Beysens, D.: The formation of dew, Atmospheric Research, 39, 215-237, https://doi.org/10.1016/0169-8095(95)00015-J, 1995.

Cai, R., Yang, D., Fu, Y., Wang, X., Li, X., Ma, Y., Hao, J., Zheng, J., and Jiang, J.: Aerosol surface area concentration: a governing factor in new particle formation in Beijing, Atmos. Chem. Phys., 17, 12327-12340, 10.5194/acp-17-12327-2017, 2017.

Groh, J., Slawitsch, V., Herndl, M., Graf, A., Vereecken, H., and Putz, T.: Determining dew and hoar frost formation for a low mountain range and alpine grassland site by weighable lysimeter, Journal of Hydrology, 563, 372-381, 10.1016/j.jhydrol.2018.06.009, 2018.

Kotzen, B.: Innovation and evolution of forms and materials for maximising dew collection, Ecocycles, 1, 39-50, 10.19040/ecocycles.v1i1.33, 2015.

Liu, Z., Wang, Y., Costabile, F., Amoroso, A., Zhao, C., Huey, L. G., Stickel, R., Liao, J., and Zhu, T.: Evidence of Aerosols as a Media for Rapid Daytime HONO Production over China, Environmental Science & Technology, 48, 14386-14391, 10.1021/es504163z, 2014.

Nilsson, T. M. J., Vargas, W. E., Niklasson, G. A., and Granqvist, C. G.: Condensation of water by radiative cooling, Renewable Energy, 5, 310-317, https://doi.org/10.1016/0960-1481(94)90388-3, 1994.

Vuollekoski, H., Vogt, M., Sinclair, V. A., Duplissy, J., Järvinen, H., Kyrö, E. M., Makkonen, R., Petäjä, T., Prisle, N. L., Räisänen, P., Sipilä, M., Ylhäisi, J., and Kulmala, M.: Estimates of global dew collection potential on artificial surfaces, Hydrol. Earth Syst. Sci., 19, 601-613, 10.5194/hess-19-601-2015, 2015.

Wang, G., Zhang, R., Gomez, M. E., Yang, L., Levy Zamora, M., Hu, M., Lin, Y., Peng, J., Guo, S., Meng, J., Li, J., Cheng, C., Hu, T., Ren, Y., Wang, Y., Gao, J., Cao, J., An, Z., Zhou, W., Li, G., Wang, J., Tian, P., Marrero-Ortiz, W., Secrest, J., Du, Z., Zheng, J., Shang, D., Zeng, L., Shao, M., Wang, W., Huang, Y., Wang, Y., Zhu, Y., Li, Y., Hu, J., Pan, B., Cai, L., Cheng, Y., Ji, Y., Zhang, F., Rosenfeld, D., Liss, P. S., Duce, R. A., Kolb, C. E., and Molina, M. J.: Persistent sulfate formation from London Fog to Chinese haze, Proceedings of the National Academy of Sciences, 113, 13630-13635, 10.1073/pnas.1616540113, 2016.

Wentworth, G. R., Murphy, J. G., Benedict, K. B., Bangs, E. J., and Collett Jr., J. L.: The role of dew as a night-time reservoir and morning source for atmospheric ammonia, Atmos. Chem. Phys., 16, 7435-7449, 10.5194/acp-16-7435-2016, 2016.

Wohlfahrt, G., Sapinsky, S., Tappeiner, U., and Cernusca, A.: Estimation of plant area index of grasslands from measurements of canopy radiation profiles, Agric. For. Meteorol., 109, 1-12, https://doi.org/10.1016/S0168-1923(01)00259-3, 2001.

The authors gratefully thank the reviewer for the comments and suggestions. We have revised our manuscript according to the reviewer's suggestions and comments. **All the changes and responses to the reviewers' comments are listed below point-by-point in blue according to a new line numbering in the revised manuscript. The major changes are highlighted with green in the revised manuscript.**

Comments to the revised manuscript by Ren et al.

In their second revised manuscript Ren et al. considered most concerns of the two reviewers. Find below further comments, first to their answers to the reviewer's comments and then to the revised manuscript and the SI.

Some answers were not convincing for me (see below) – here the editor should find a final decision. In contrast several minor points could be easily corrected in a final version. However, caused by the significant amount of text (answers, manuscript, SI) and this third correction, I do not want to see a further version again.

Major Concerns (see answers to the reviewer's comments):

Reviewer #1:

1) Calculated NO2 uptake coefficients for particles surfaces:

In the revised version the authors corrected the particle surface area leading to more reasonable theoretical uptake coefficient if all HONO formation would take place on the particles. However first, the range of S/V in the very clean environment of Melpitz (see lines 286-292 main text…) is still in the same range than values published for one of the most polluted environments of the word, i.e. Beijing. This is highly unreasonable. Please check again and at least, give any explanation for these high values (sand storms?). Lower S/V would further increase the theoretical NO_2 uptake coefficient.

Response: As the reviewer suggested, we checked the measured particle size distribution and recalculated the particle surface density S_a again, no error was found for the S_a calculation. We should mention that the reported S_a values of (5.1-9.9) $\times 10^{-4}$ m^2 m^{-3} and RH corrected value of (0.6-1.9)$\times 10^{-3}$ m^2 m^{-3} in lines 417 and 420 (previous version) correspond only the night-time period 18:00-22:00 (UTC) since only nighttime data was used to calculate the HONO formation through heterogeneous conversion of NO_2. As shown in Figure R1 (we also add it in SI as Figure S5b), the S_a values ranged from 4.2×10^{-5} to 9.9×10^{-4} m^2 m^{-3} for whole day period during our field measurement period of April 19th -29th 2018. This value is one order magnitude lower than S_a value of 0.2-3.4$\times 10^{-3}$ m^2 m^{-3} in Beijing (Liu et al., 2014;Wang et al., 2016). However, due to the high RH (RH ~100% during nighttime in Figure R1), the S_a values would be strongly enhanced by the RH correction (Figure R1) to be (0.5-1.9)$\times 10^{-3}$ m^2 m^{-3}. For the clarity, we improve the sentence as "The particle surface

density S_a was calculated as (0.4-9.9) $\times 10^{-4}$ m^2 m^{-3} from the particle size distribution (Figure S5a) ranged from 5 nm to 10 μm of APSS and D-MPSS data by assuming the particle are in spherical shape for the whole day period of April 19th-29th 2018. Due to the high RH (RH ~100% during nighttime in Figure S5b), the particle surface density S_a would be strongly enhanced (by one order magnitude) by the RH correction to be (0.5-1.9) $\times 10^{-3}$ m^2 m^{-3} with a hygroscopic factor f(RH) following the method of Li et al. (2012) and Liu et al. (2008)" in line 416-421."

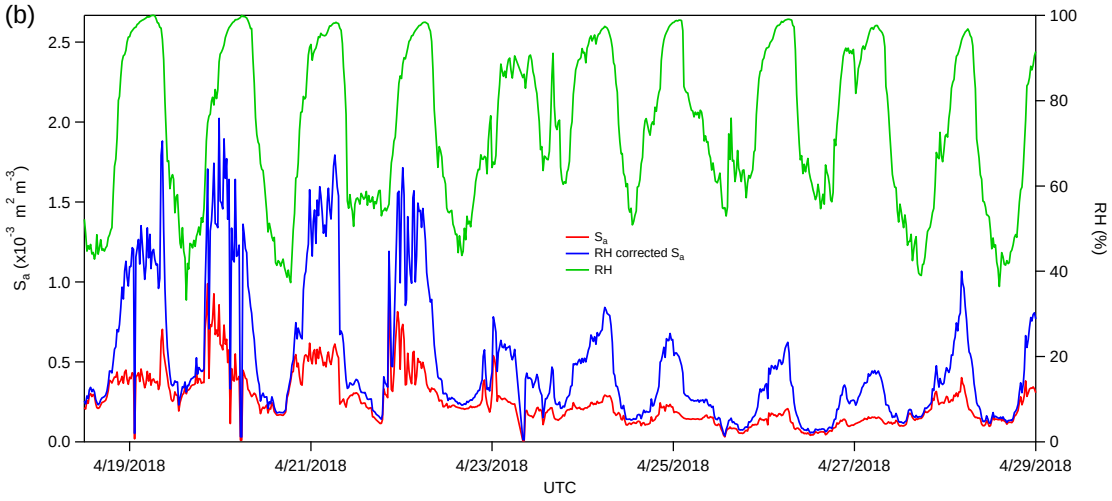

Figure R1. The particle surface density S_a and RH corrected S_a value calculated from the particle size distribution for our field measurement period of April 19th-29th 2018.

Second, still the authors do not well describe (or understand?) the main conclusion from this section (see their answer. "This theoretical uptake coefficient falls into a reasonable range of…"), which becomes even more obvious considering the answer to the same point for reviewer 2 ("… similar to former studies, which normally is regarded as unimportant for the HONO formation…"). If the uptake were as high (>10^-4), than HONO would be formed on the particles and this mechanism would be certainly important!

The correct interpretation is however:
The average uptake of NO2 in the dark which the authors now calculate is 1.7x10^-4. This number is 2-3 orders of magnitude higher than typical uptake coefficients determined in the lab for the uptake of NO2 in the dark (!) on different substrates (e.g. R2/Teflon/glass/NaCl/TiO2/etc.: some 10^-7 to 10^-8, R4/soot/SS: 10^-6 to <10^-8, R4/phenols: ca. 10^-6, …). There is no study were a dark (!) uptake of 10^-4 was determined, except for fresh soot for the first seconds of reaction (later passivation, s. above). Thus, the calculations given by the authors (and the theoretical uptake would be even higher for realistic S/V, see above) clearly shows that formation on particles is not important, in agreement with their own conclusions in the manuscript. This should be made clear now.

Response: We thank the reviewer for the correction. We have replaced the sentence:
"the calculated $\gamma_{NO2\rightarrow HONO\_a}$ from the Eq. 4 varied from 2.8×10^{-5} to 3.8×10^{-4} with a mean value of $(1.7\pm1.0)\times10^{-4}$. This theoretical uptake coefficient falls into a reasonable range of 10^{-6} - 10^{-4} similar to former studies (Kleffmann et al., 1998;Kurtenbach et al., 2001;Wong et al., 2011;VandenBoer et al., 2013). However, considering the weak correlations between $HONO_{corr}$ (R^2=0.566), $HONO_{corr}$/ NO_2 (R^2=0.208) and S_a (Figure S6), the relative amount of HONO formed on particle surfaces might be small as previously reported (Wong et al., 2011;Sörgel et al., 2011;Kalberer et al., 1999)." by:
"the calculated $\gamma_{NO2\rightarrow HONO\_a}$ from the Eq. 4 varied from 2.8×10^{-5} to 3.8×10^{-4} with a mean value of $(1.7\pm1.0)\times10^{-4}$. This number is 2-3 orders of magnitude higher than typical uptake coefficients determined in the lab for the uptake of NO_2 in the dark on different substrates, e.g. Teflon/glass/NaCl/TiO_2/soot/Phenol etc: 10^{-6} to $<10^{-8}$ (Kleffmann et al., 1998;Kurtenbach et al., 2001;Ammann et al., 1998;Gutzwiller et al., 2002). Thus, this theoretical uptake coefficient clearly shows that formation on particles is not important. In addition, the weak correlations between $HONO_{corr}$ (R^2=0.566), $HONO_{corr}$/ NO_2 (R^2=0.208) and S_a (Figure S6) confirm that the HONO formed on particle surfaces could be unimportant as previously reported (Wong et al., 2011;Sörgel et al., 2011;Kalberer et al., 1999)." in line 431-440.

2) Explanation of the morning HONO peaks by dew water nitrite.

I still cannot follow the use of the enhancement factor for the dew nitrite. First, I do not think that the dew volume follows perfect linearly the available surface area on the ground and I still think the volume of humid air getting into contact will also control the dew formation. This is an important point which should be verified by other studies since a correction of the amount of nitrite (=> HONO morning peak) is increased by a factor of 12!

Response: Firstly we agree with the reviewer that the volume of humid air getting into contact will also control the dew formation. But more dew could be formed if there is more cold surface area in contact with certain amount of humid air, this has been well described by Kotzen (2015). In other words, we could collect more dew (larger volume of dew (V_{dew})) if we used for example a dew sampler with corrugations on one side than a flat dew sampler. This is also the case of the nature, larger area of leaves of grasses than, for example, 1 m^2 of ground surface could strongly enhance the dew formation. Hence, the V_{dew} obtained from the collector is not necessarily representative of V_{dew} that forms naturally on the grassland canopy because of their different cold contacted surface area with humid air (Wentworth et al., 2016;Groh et al., 2018).
Secondly, we also agree with the reviewer that dew volume cannot follow perfect linearly the available surface area on the ground. Hence in this version, we assumed an enhanced factor of

2 ×LAI as 1-6 to take the areas on both sides of the leaves and the vegetation-covered areas on the ground into account. We strongly point out here, that this enhanced factor is an assumption. The collection of dew is increasingly focused in several studies within the last years (Jacobs et al., 1999;Takenaka et al., 2003;del Campo et al., 2006;Ye et al., 2007;Guan et al., 2014;Kotzen, 2015;Vuollekoski et al., 2015;Groh et al., 2018) as dew is expected to form a natural reservoir of reactive tropospheric species at night. An exact evaluation or comparison of the volume between an artificial dew collector and the "real" dew on grasses was not performed yet. This is an important question that has to be answered in future studies.

The discussion in Section 4.3.3 was changed to "…α was calculated as 2 ×LAI to take the areas on both sides of the leaves and the vegetation-covered areas on the ground into account. And a factor of 6 for LAI was assumed and used in section 4.2.2. However, regarding the possibly different grass height during the HONO field measurement and dew measurements in April 2018 and May 2019, respectively, we would use a range of 1-6 for LAI in this section. During the HONO peak at 6 or 7 UTC, the mixing height ranged between 175 m and 600 m, while the mixing height ranged from 20 m to 200 m at 0:00 – 5:00 UTC. Hence, the overall concentration increase from this source would be 377-2264, 189-1132, 76-122, 38-226 and 13-76 pptv, if all of the deposited HONO is released into the overlying air column for a mixing height of 20, 40, 100, 200 and 600 m, respectively. Since the released HONO was subjected to photolysis, using a J_{HONO} from TUV model scaled by global radiation (section 2.7), a maximum [HONO] of 176-1053, 88-527, 35-211, 18-105 and 6-35 pptv for the mixing height 20, 40, 100, 200 and 600 m, respectively, would be contributed from the surface nitrite release at 7:00 UTC after the process started from 4:00 UTC. For a reasonable 100 m mixing height, this would account for 5-30% of the observed HONO morning peak in Figure 6. This low percentage might be a result of the different sampling time of dew measurement compared with HONO measurement and further studies are required for the exact quantification. …"

Second, even if the authors are right with the increasing dew volume on grass (x12) than for increasing volume of the dew water the resulting liquid concentration of nitrite would be 12 times lower than on the glass substrates used, since the amount of HONO in the mixing layer will control the soluble nitrite (see the assumptions by the authors using the H in their equations…). Thus, the amount of dew nitrite is for sure strongly overestimated.

Response: Since the surface area of our glass sampler is only 1.5 m^2, which is much smaller than the grass area around the Melpitz station and cannot affect the bulk volume of dew water on the grass around the Melpitz station. Hence, our measured liquid concentration of nitrite on the collector can represent the nitrite concentration in dew water on the grass. But V_{dew} obtained from the collector is not necessarily representative of V_{dew} that forms naturally on

the grassland canopy because of their different cold contacted surface area with humid air (Wentworth et al., 2016). Hence, in this version, an enhanced factor of 2×LAI with LAI values in the range of 1-6 would help to represent the V_{dew} on the grassland canopy from the measure V_{dew} on the collector. However, according to the observed grass height during the campaign, a LAI value of 6 would be preferred regarding the publication of Wohlfahrt et al. (2001).

Now even with this 12 times too high nitrite, considering HONO photolysis (this is done very well now!) and using a reasonable mixing height of H=100 m in the morning (two hours after sunrise!) only 30 % of the HONO morning peaks observed can be explained and this would be <3 % for a reasonable amount nitrite in dew!

So although I can follow qualitatively the author's explanation of the experimental data (peak HONO when rh decrease…) the quantitative explanation is not valid. And the main point is most probably that the authors compare data of two different years (apples and oranges…).

Response: We agree with the reviewer that the main point for this low value (5-30% in this version) is most probably that we compared data of two different years, and we already mention it in line 661-663 "This low percentage might be a result of the different sampling time of dew measurement compared with HONO measurement." We should although mention that this is a first assumption with qualitative results and further studies are required for the exact quantification.

Reviewer #2:

1) Details to the MARGA:

In their answer to the accuracy of the MARGA the authors specify:
"For the accuracy of the ion chromatography system, liquid NO2- standards were twice injected to the MARGA with concentrations of 70, 120 and 150 µg L-1. The resulting slope of 1.13 (R2 = 0.99) indicates slightly lower measured NO2- concentrations …"
I do not understand that section? Was the raw data of the IC of the two injections plotted against each other (70/70, 120/120, 150/150) and the slope was 1.13? In this case the precision (!) is only 13 %!? Or was nitrite injected into the rotated denuder under zero air (complete system check…) and compared with the direct calibration of the IC only (I expect the latter, but the first is mentioned in the text…).

Response: We are sorry for this confusion. We tested the ion chromatography by injecting standard solutions with defined NO_2^- concentrations of 70, 120 and 150 µg L. The correlation

between both the predefined concentrations and the measured concentrations by the MARGA IC resulted in a slope of 1.13. The MARGA is internally calibrated by an LiBr solution. Hence, no calibration solutions were needed for the MARGA measurements. We will improve the description in the main manuscript as follows:

"To test the robustness of the ion chromatography within the MARGA, standard solutions with defined NO_2^- concentrations of 70, 120 and 150 µg L^{-1} were injected in the IC system. The correlation between both the predefined concentrations within the standard solutions and the measured concentrations by the MARGA IC resulted in a slope of 1.13. This value…" in line 157-161.

Than for the blank tests the authors mention that the first two hours of the samples were not considered because of "still … residual concentrations". Here the authors should give a true response time of the instrument which is than clearly longer than the one hours sample time. This would also help to understand some differences in the timing of the signals of the two instruments mentioned by reviewer#2 below. If the true response time is e.g. two hours, than use the same averaging for the LOPAP when comparing both instruments (this may further decrease the noise of the intercomparsion data…).

Response: The response time of both instruments is fast. The MARGA output gives high concentrations within the same hour. However, it is expected that the residual concentrations of the previous hour, which might be in maximum 10 %, could be added to the real atmospheric concentrations of the current hour. This would lead to less sharp concentrations courses.
We tested the correlation between MARGA and LOPAP for both measurement periods and shifted the hourly concentrations of the MARGA one and two hours back and forward regarding the LOPAP concentrations. The high correlation (R^2) described in Figure 1 decreased strongly to values below 0.5 when the MARGA concentrations were shifted one hour and decreased below 0.3 for a shift of two hours.
Hence, the correlation described in Figure 1 and in the main manuscript gives the best results.

2) Details to the LOPAP:

Typically the LOPAP instrument has a time response of 5 min. In this case the authors cannot specify a DL for a time resolution of 30 s (one data point collected?)!
In addition, I cannot understand why the authors obtained a detection limit of only 0.1 ppt using the zero noise of 30 min data (2 sigma or 3 sigma?). The lowest DL of the instrument which I saw was 0.2 ppt (see line 92) by the group who developed the instrument and using extreme experimental conditions (very long optical path length, high gas flow etc., see

Kleffmann and Wiesen, 2008). The authors should explain how they obtained this outstanding DL (or correct it to the typical 1-2 ppt, I am sure this is again an error…).

Response: We thank the reviewer for the correction. The detection limit was correct in line 181-182 "The detection limit of LOPAP was approximately 1-2 pptv with a response time of 5 min."

3) New weighted regression of the intercomparison data:
While the slope of the intercomparison for M1 did not significantly change, the slope for M2 is now only 1.66 und not 1.9 from the former versions, which is significant!? Is that only caused by a weighted/non-weighted regression? Both data sets correlate very well with no large outliers. Thus even if outliers have larger relative errors than other points (and for me the relative errors (%) look the same for all data, in this case a weighted is similar to a non-weighted orthogonal regression…) than the slope should not change too much (see M1). Please check the data again.

Response: As the reviewer suggested, we carefully checked the data. We again performed the calculation of the unweighted (values in the first manuscript version) and the weighted (values in the revised manuscript version) Deming regression. In case of the unweighted version, we again received for M1 a slope of 1.58±0.08 and an intercept of 29±33 pptv. For period M2, the slope and intercept were 1.90±0.07 and 120±16 pptv, respectively. For the weighted case, the slopes increased to 1.71±0.08 and 2.17±0.09 for M1 and M2, respectively. The intercept was -15±21 and 79±10 pptv for M1 and M2, respectively. The correlation in both periods were significant ($p < 0.001$). We are sorry for the wrong values in the last version, and the right values were added in line 263-265 "The comparisons of the MARGA and LOPAP HONO measurements for period M1 and period M2 in Figure 1c result in slopes of 1.71 and 2.17 using error weighted Deming regression, respectively." and 272-273 "… which could account for ca. 71% (M1, where both LOPAP and MARGA used the common MARGA inlet) of these ca. 117% of overestimated HONO measurement from MARGA. Additional artefacts such as heterogeneous formation of HONO due to the long MARGA inlet system should be responsible for another ca. 46% (the difference between slopes M2 and M1). …"

Concerns to the revised manuscript:

The following concerns are listed in the order how they appear in the manuscript.

Lines 25-27: The authors should correct this number to 30 % (or <3%, see major concern), see their calculations to the dew nitrite…

Response: We should mention that the "percentage of 90-100%" in line 26 was obtained from the chemical model. As the reviewer mentioned above, the number of 5-30% is most probably due to the fact that we compared data of two different years, further field measurement will be planned.

Line 75-76: Just a comment (no correction), yes I agree, but in this study there is also no simultaneous data…

Response: The sentence of "Few of them have simultaneously quantified both dew and atmospheric composition." was removed.

Line 158-162: see above

Response: We changed the text according to our answer in the major comments.

Line 181: see above

Response: This part was corrected to "The detection limit of LOPAP was approximately 1-2 pptv with a response time of 5 min." in line 181-182.

Lines 254-255: No, if you consider the 1 h data, also the peak values of the LOPAP are lower. And it is trivial that the high resolution data peaks of the LOPAP are higher! In Fig 1a) apples (30 s data LOPAP) and oranges (1h data Marga) are compared!

Response: The Figure 1a used to show the original measured data (not averaged) for both instruments: LOPAP and MARGA, and the high time resolution data of LOPAP could present us more clearly time evolution of HONO in the early morning rather than MARGA. We corrected the sentence of "It indicates that the MARGA values were higher than the values of LOPAP but not during the peak events" to "It indicates that the MARGA values were higher than the values of LOPAP".

Line 255-261: check for the lower time response of the Marga and correct text accordingly (when averaging the LOPAP data for two hours, most probably the differences disappear…).

Response: An averaging of the LOPAP and MARGA values for two hours resulted in low deviation in the regression lines.

M1: $y=(1.59 \pm 0.09)x+(27 \pm 34)$ ← unweighted $(R^2 = 0.945)$

M1: y=(1.69±0.08)x+(-7±21) ← weighted

M2: y=(1.99±0.10)x+(103±20) ← unweighted (R^2 = 0.818)
M2: y=(2.18±0.08)x+(74±21) ← weighted
Hence, the response time for both instruments is reasonable. We corrected the values in lines 263-265 "The comparisons of the MARGA and LOPAP HONO measurements for period M1 and period M2 in Figure 1c result in slopes of 1.71 and 2.17 using error weighted Deming regression, respectively."

Line 264: see above

Response: We changed the values according to our answer in the major comment.

Line 275: this was more than 30 % in the former versions. Conclusions would change: if the data is correct (s. above?) than formation in the inlet is not too significant and in between the combined errors…

Response: The corrected value of 46% was added in lines 273-275 "Additional artefacts such as heterogeneous formation of HONO due to the long MARGA inlet system should be responsible for another ca. 46% (the difference between slopes M2 and M1)."

Line 290 and 294: Give either the average or the median for both…

Response: The HONO average value of 162±96 pptv and 254±114 pptv during daytime and nighttime, respectively, were provided in line 294.

Lines 310-327: The different cases a-c are not very clear here. I would first sum up the three cases in short sentences (see lines 570-573) and then explain in more detail…

Response: This section was changed to "Such daytime pattern was also found in Spain, for a site surround by forests and sandy soils (Sörgel et al., 2011). Sörgel et al. (2011) explained this by local emissions, which are trapped in the stable boundary layer before its breakup of the inversion in the morning based on a similar diurnal cycle for NO and NO_2, which is different with this work. In this work, the NO_2 mixing ratio decreased from the midnight until noon and NO peaked at 5:00 (UTC) then kept low concentration (<1 ppbv) for 18 hours of one day. However, three hypotheses could be expected to explain this HONO morning peak: hypothesis (a) of HONO morning peak might possibly be caused by the photolysis of particle-phase HNO_3/NO_3^- (Zhou et al., 2003;Ye et al., 2016;Zhou et al., 2011), since as shown in Figure 4a, 4e and 4f, the early morning variation trend of HONO during daytime

was similar to the one of NH_3 in the gas phase as well as NO_3^- and NH_4^+ in PM_{10}. Hypothesis (b), as reported by Stemmler et al. (2006), the photosensitized NO_2 on humic acid could act as a source of HONO during the daytime. For hypothesis (c), this morning peak of HONO has been reported for Melpitz (April 4th-14th, 2008) by Acker et al. (2004), who expected that the storage of HONO on wet surfaces can be a source for observed daytime HONO. Exactly, it was observed that dew was formed overnight during our campaign in Melpitz. Gaseous HONO could be deposited in these droplets. Due to evaporation after sunrise, HONO would be reemitted in the atmosphere and lead to a HONO morning peak. These hypotheses will be further discussed in Section 4.".

Line 331: …species or by the hetero…

Response: "by' was added in line 330.

Line 420: see above

Response: This part in lines 416-421 was changed to "The particle surface density S_a was calculated as (0.4-9.9) $\times 10^{-4}$ m^2 m^{-3} from the particle size distribution (Figure S5a) ranged from 5 nm to 10 µm of APSS and D-MPSS data by assuming the particle are in spherical shape for the whole day period of April 19th-29th 2018. Due to the high RH (RH ~100% during nighttime in Figure S5b), the particle surface density S_a would be strongly enhanced (one magnitude) by the RH correction to be (0.5-1.9) $\times 10^{-3}$ m^2 m^{-3} with a hygroscopic factor f(RH) …" according to the major concern.

Lines 433-438: see above.

Response: This part in lines 433-440 was changed to "This number is 2-3 orders of magnitude higher than typical uptake coefficients determined in the lab for the uptake of NO_2 in the dark on different substrates, e.g. Teflon/glass/NaCl/TiO_2/soot/Phenol etc: 10^{-6} to $<10^{-8}$ (Kleffmann et al., 1998;Kurtenbach et al., 2001;Ammann et al., 1998;Gutzwiller et al., 2002). Thus, this theoretical uptake coefficient clearly shows that formation on particles is not important. In addition, the weak correlations between $HONO_{corr}$ (R^2=0.566), $HONO_{corr}$/ NO_2 (R^2=0.208) and S_a (Figure S6) confirm that the HONO formed on particle surfaces could be unimportant as previously reported (Wong et al., 2011;Sörgel et al., 2011;Kalberer et al., 1999)." according to the major concern.

Lines 461-462: The sentence makes no sense? "…uptake coefficient …is lower than the reactive surface…" (apples and oranges…).

Response: The sentence of "It should be noted here that the obtained NO_2 uptake coefficient on the ground surface is lower than the reactive surface provided by aerosols." has been removed.

Line 481: Please check for that average number of 0.16 ppb/h. If I take the average data shown in Fig. 4 a (decreasing HONO from 20:00-4:00), I get an HONO uptake of only 0.033 ppb/h, nearly four times lower?

Response: The average number of 0.16 ppb/h was well confirmed. However, we should correct previous Eq.7 of $L_{HONO}=\frac{d[HONO]}{dt} - k_{het} \times [NO_2]$ to "$L_{HONO}=\frac{d[HONO]}{dt} + k_{het} \times [NO_2]$" for the wrong typing.

We calculated the HONO deposition rate (L_{HONO}) for each day of our field measurement as below in the Table R1:

Table R1, Calculated HONO deposition rate (L_{HONO}) during nighttime for our field measurement period of April 19th-29th 2018.

Date	UTC	L_{HONO} (ppbv h^{-1})
19/04/2018	19:51-4:00	0.45
20/04/2018	19:31-4:00	0.21
21/04/2018	20:31-4:00	0.09
22/04/2018	21:21-4:00	0.14
23/04/2018	18:51-4:00	0.04
24/04/2018	17:51-4:00	0.14
25/04/2018	21:21-4:00	0.09
26/04/2018	18:31-4:00	0.07
27/04/2018	22:41-4:00	0.11
28/04/2018	19:50-4:00	0.28
Average		0.16±0.12

Eq. 8: delete the "ground" for the velocity of HONO (this is a gas kinetics number…)

Response: The "ground" was deleted for Eq. 8, 12, 13, 14, 15, 16 and also line 494.

Line 506: should by microgram per Liter and not mg/L!

Response: "mg L^{-1}" was corrected to "μg L^{-1}" in line 507.

Lines 515-530: please check again for HONO, see below SI

Response: We carefully checked the gas phase diffusion coefficient for HONO and explained below in SI.

Line 521-523: I do not understand the second part of the sentence, since Rb is no function of the WS, see Fig. S9.

Response: We are sorry for the uncorrected description, "especially when the winds speed is smaller than ~1 m s^{-1}." was removed.

Line 536-537: No, R2 and R7 are not very important. The dark conversion of NO2 is 1-2 orders of magnitude less efficient than the daytime conversion of NO2 (see e.g. Kleffmann et al., 2005) and typically NO+OH makes only 10 % of the daytime HONO (see same study, where OH and J(HONO) were measured...). See also own conclusion in line 566…

Response: We thank the reviewer for the correction, and we changed the sentence to "the R2 and R7 are not expected to be responsible for this HONO morning peak, but could contribute to the daytime HONO for the period of 10:30-16:30 (UTC)." ln line 535-536.

Line 549 and others: Typically capital letters are used for PSS (or use pss but not Pss…).

Response: "Pss" was corrected to "PSS" in line 548 and Figure 6.

Line 557: better refer to "model 1" (see legend of Figure 6) since the colours are not easily visible (red/orange/pink…)

Response: We added "Model 1" in line 556 to clarify it.

Line 625: "… respectively (see Table 4) with an average of…" You do not find the average in table 4…

Response: We added the average value of 0.016±0.014 pptv $\%^{-1}$ s^{-1} in Table 4 as below:

Table 4. Summary of the temporary HONO emission rate from dew water, $k_{emission}$ from April 19th to 29th, 2018.

Period	$k_{emission}$ (pptv $\%^{-1}$ s^{-1})	
	Min	Max
21/4/2018	0.0054	0.0357
22/4/2018	0.0048	0.0314
24/4/2018	0.0057	0.0192

26/4/2018	0.0067	0.0302
27/4/2018	0.0048	0.0215
28/4/2018	0.0079	0.017
mean	0.006 ±0.001	0.026 ±0.008
Total average	0.016 ±0.014	

Lines 632-635 and Figure S11: Please check the calculations for the higher k(emission) of 0.026. The peak should be higher than the experimental peak and not lower (in Fig. S11), since an excellent agreement is obtained using the average k(emission) of 0.016 (see Figure 6)!?

Response: We thank the reviewer for the correction, we corrected the Figure S11 as below.

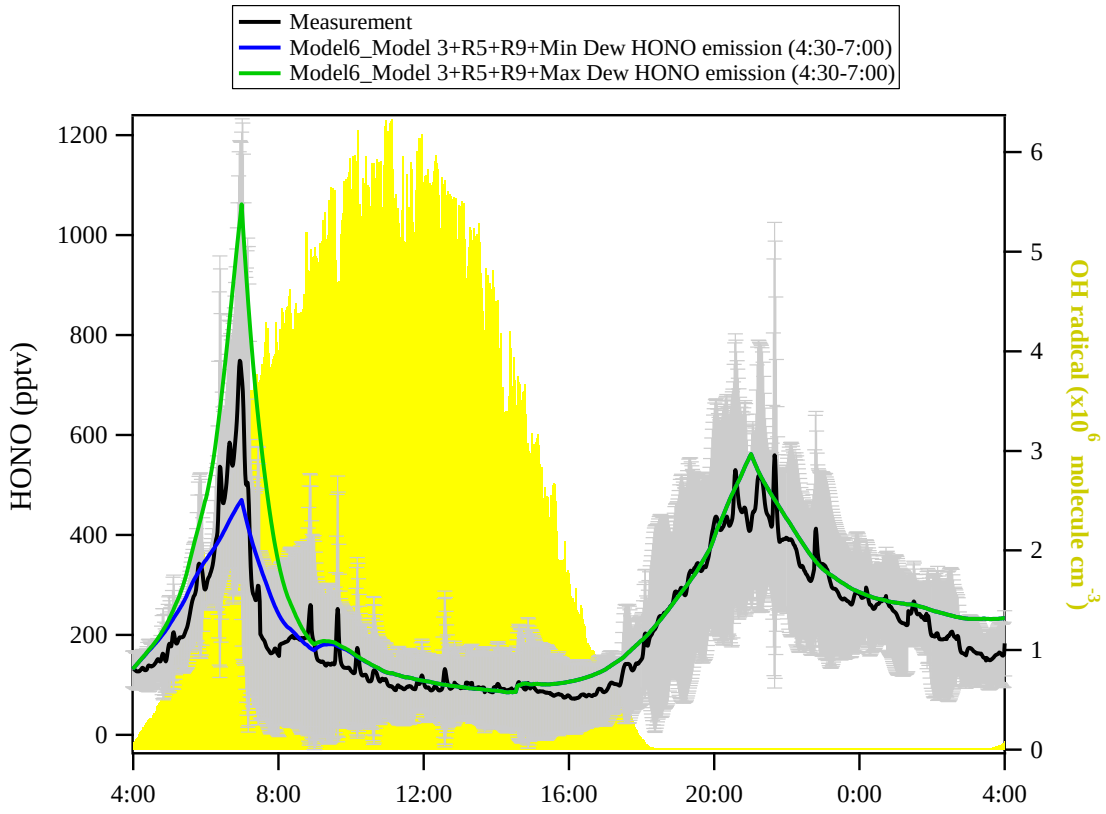

Figure S11. Observed average HONO atmospheric concentration (black line, ±1σ in shaded area) and the calculated HONO concentration in model 6 using a min dew HONO emission $k_{emission}$ = 0.006 pptv $\%^{-1}$ s^{-1} (blue line) and max dew HONO emission $k_{emission}$ = 0.026 pptv $\%^{-1}$ s^{-1} (green line), respectively.

Section 4.3.3: see above, correct the 30% to <3 % and change all the discussion...

Response: The discussion was changed to "…α was calculated as 2 ×LAI to take the areas on both sides of the leaves and the vegetation-covered areas on the ground into account. And a factor of 6 for LAI was assumed and used in section 4.2.2. However, regarding on the possibly different grass height during the HONO field measurement and dew measurements in April 2018and May 2019, respectively, we would use a range of 1-6 for LAI in this section. During the HONO peak at 6 or 7 UTC, the mixing height ranged between 175 m and 600 m, while the value ranged from 20 m to 200 m at 0:00 – 5:00 UTC. Hence, the overall concentration increase from this source would be 377-2264, 189-1132, 76-122, 38-226 and 13-76 pptv, if all of the deposited HONO is released into the overlying air column for a mixing height of 20, 40, 100, 200 and 600 m, respectively. Since the released HONO was subjected to photolysis, using a J_{HONO} from TUV model scaled by global radiation (section 2.7), a maximum [HONO] of 176-1053, 88-527, 35-211, 18-105 and 6-35 pptv for the mixing height 20, 40, 100, 200 and 600 m, respectively, would be contributed from the surface nitrite release at 7:00 UTC after the process started from 4:00 UTC. For a reasonable 100 m mixing height, this would account for 5-30% of the observed HONO morning peak in Figure 6. This low percentage might be a result of the different sampling time of dew measurement compared with HONO measurement and further studies are required for the exact quantification. …" in section 4.3.3.

Line 722: "…direct estimation …" see many assumptions…

Response: "… direct evaluation" was changed to "direct estimation".

Table caption 3: "…during early nighttime."

Response: "… during nighttime" was corrected to "… during early nighttime".

Fig. 1: Check for the correct slope and the averaging time of the LOPAP (= time response MARGA).

Response: See above.

Figure caption 6: PSS

Response: "Pss" was corrected to "PSS" in the caption of Figure 6.

Figure 7: Specify which data is shown for the linear regressions (22th April for the low slope and 24th April for the high slope?)

Response: The caption of Figure 7 was corrected to "Example of $\frac{HONO_{unknown}}{99.5-RH}$ as a function of time (zero point from time 4:30, UTC) to estimate the temporary HONO emission rate from dew water ($k_{emission}$). Blue line is the linear least-square analysis of $\frac{HONO_{unknown}}{99.5-RH}$ vs. internal time to obtain the minimum (e.g. 22th April for the low slope) and maximum (e.g. 24th April for the high slope) of $k_{emission}$, respectively.".

SI Resistance model/Figure S9:

The authors should check the diffusion coefficient of HONO (the one for NO2 is correct, but I do not have data for HONO). Here the slightly heavier molecule HONO has a much high diffusion coefficient than NO2, which is not plausible (Is that data for low pressure?). Even the diffusion coefficient of NO (30 g/mol) is much lower than the value given for HONO. This will change all discussion on the transport limited uptake of HONO (the blue line will be ca. near the yellow line), which will get important at much more conditions (for gammas >10^-6…), also making the assumption of using the whole mixing layer for the HONO uptake more unreasonable.

Sorry I did not realize this point during the last review (massive work…).

Response: Hirokawa et al. (2008) investigated the uptake kinetics of gas phase HONO by a pH-controlled aqueous solution by using a wetted wall flow tube. They found that the uptake rate of the gaseous HONO depends on the pH of the solution. For the uptake by neutral (pH=7.1) and alkaline (pH=11.1) solutions, the gas phase concentration was observed to decay exponentially, suggesting that the uptake was fully limited by the gas phase diffusion. On the other hand, the uptake by the acidic solution was found to be determined by both the gas phase diffusion and the liquid phase processes such as physical absorption and reversible acid dissociation reaction. Finally, Hirokawa et al. (2008) determined the gas phase diffusion coefficient for HONO in the carrier gas mixtures (Dg) as $5.7 \pm 0.5 \times 10^{-5}$ m^2 s^{-1} 294 K and 760 Torr, however, they assumed the aqueous phase diffusion coefficient of HONO, D_{aq}, to be equal to D_{aq} for NO_2 at 298 K. In our previous version, we used the value of 7.2×10^{-5} at 660 torr as the study of VandenBoer et al. (2013). Now we recalculate the molecular diffusion resistance R_b using the gas phase diffusion coefficient of $5.7 \pm 0.5 \times 10^{-5}$ m^2 s^{-1} as shown in new Figure S9. As shown in new Figure S9, the current calculation will not change the discussion on the transport limited uptake of HONO.

In addition, as we already mentioned in the section of "Investigating resistance limitations in transport of HONO and NO_2 to the ground surface during the Melpitz measurement" of SI, the surface layer height was set to 15 m as example for nighttime values in Melpitz not the whole mixing layer.

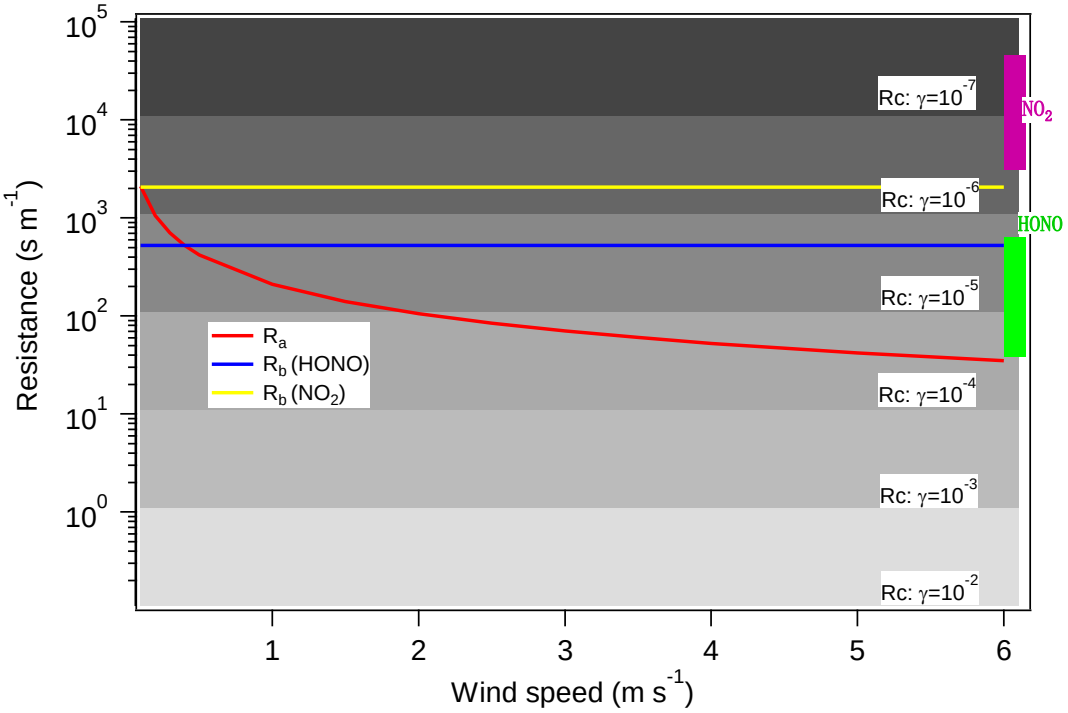

Figure S9. Estimated contributions of resistance parameters to the observable ground surface processes for the HONO and NO_2 uptake values derived from Melpitz station. A series of grey shaded regions define the borders of the reactive uptake resistance (R_c), the R_c values calculated from upper and lower limit uptake values of HONO and NO_2 in this work are shown in green and pink column, respectively. The aerodynamic transport resistance (R_a, red line) and diffusion resistance (R_b, blue line for HONO and yellow for NO_2) are shown in the Figure."

References

Acker, K., Spindler, G., and Bruggemann, E.: Nitrous and nitric acid measurements during the INTERCOMP2000 campaign in Melpitz, Atmos. Environ., 38, 6497-6505, 10.1016/j.atmosenv.2004.08.030, 2004.

Ammann, M., Kalberer, M., Jost, D. T., Tobler, L., Rössler, E., Piguet, D., Gäggeler, H. W., and Baltensperger, U.: Heterogeneous production of nitrous acid on soot in polluted air masses, Nature, 395, 157, 10.1038/25965, 1998.

del Campo, A. D., Navarro, R. M., Aguilella, A., and González, E.: Effect of tree shelter design on water condensation and run-off and its potential benefit for reforestation establishment in semiarid climates, For. Ecol. Manag., 235, 107-115, https://doi.org/10.1016/j.foreco.2006.08.003, 2006.

Groh, J., Slawitsch, V., Herndl, M., Graf, A., Vereecken, H., and Putz, T.: Determining dew and hoar frost formation for a low mountain range and alpine grassland site by weighable lysimeter, Journal of Hydrology, 563, 372-381, 10.1016/j.jhydrol.2018.06.009, 2018.

Guan, H., Sebben, M., and Bennett, J.: Radiative- and artificial-cooling enhanced dew collection in a coastal area of South Australia, Urban Water Journal, 11, 175-184, 10.1080/1573062X.2013.765494, 2014.

Gutzwiller, L., Arens, F., Baltensperger, U., Gäggeler, H. W., and Ammann, M.: Significance of Semivolatile Diesel Exhaust Organics for Secondary HONO Formation, Environ. Sci. Technol., 36, 677-682, 10.1021/es015673b, 2002.

Hirokawa, J., Kato, T., and Mafuné, F.: Uptake of Gas-Phase Nitrous Acid by pH-Controlled Aqueous Solution Studied by a Wetted Wall Flow Tube, J. Phys. Chem. A, 112, 12143-12150, 10.1021/jp8051483, 2008.

Jacobs, A. F. G., Heusinkveld, B. G., and Berkowicz, S. M.: Dew deposition and drying in a desert system: a simple simulation model, J. Arid Environ., 42, 211-222, https://doi.org/10.1006/jare.1999.0523, 1999.

Kalberer, M., Ammann, M., Arens, F., Gäggeler, H. W., and Baltensperger, U.: Heterogeneous formation of nitrous acid (HONO) on soot aerosol particles, J. Geophys. Res. Atmos., 104, 13825-13832, doi:10.1029/1999JD900141, 1999.

Kleffmann, J., Becker, K. H., and Wiesen, P.: Heterogeneous NO_2 conversion processes on acid surfaces: Possible atmospheric implications, Atmos. Environ., 32, 2721-2729, 10.1016/s1352-2310(98)00065-x, 1998.

Kotzen, B.: Innovation and evolution of forms and materials for maximising dew collection, Ecocycles, 1, 39-50, 10.19040/ecocycles.v1i1.33, 2015.

Kurtenbach, R., Becker, K. H., Gomes, J. A. G., Kleffmann, J., Lörzer, J. C., Spittler, M., Wiesen, P., Ackermann, R., Geyer, A., and Platt, U.: Investigations of emissions and heterogeneous formation of HONO in a road traffic tunnel, Atmos. Environ., 35, 3385-3394, 10.1016/s1352-2310(01)00138-8, 2001.

Li, X., Brauers, T., Häseler, R., Bohn, B., Fuchs, H., Hofzumahaus, A., Holland, F., Lou, S., Lu, K. D., Rohrer, F., Hu, M., Zeng, L. M., Zhang, Y. H., Garland, R. M., Su, H., Nowak, A., Wiedensohler, A., Takegawa, N., Shao, M., and Wahner, A.: Exploring the atmospheric chemistry of nitrous acid (HONO) at a rural site in Southern China, Atmos. Chem. Phys., 12, 1497-1513, 10.5194/acp-12-1497-2012, 2012.

Liu, X., Cheng, Y., Zhang, Y., Jung, J., Sugimoto, N., Chang, S.-Y., Kim, Y. J., Fan, S., and Zeng, L.: Influences of relative humidity and particle chemical composition on aerosol scattering properties during the 2006 PRD campaign, Atmos. Environ., 42, 1525-1536, https://doi.org/10.1016/j.atmosenv.2007.10.077, 2008.

Liu, Z., Wang, Y., Costabile, F., Amoroso, A., Zhao, C., Huey, L. G., Stickel, R., Liao, J., and Zhu, T.: Evidence of Aerosols as a Media for Rapid Daytime HONO Production over China, Environmental Science & Technology, 48, 14386-14391, 10.1021/es504163z, 2014.

Sörgel, M., Regelin, E., Bozem, H., Diesch, J.-M., Drewnick, F., Fischer, H., Harder, H., Held, A., Hosaynali-Beygi, Z., Martinez, M., and Zetzsch, C.: Quantification of the unknown HONO daytime source and its relation to NO_2, Atmos. Chem. Phys., 11, 10433-10447, 10.5194/acp-11-10433-2011, 2011.

Stemmler, K., Ammann, M., Donders, C., Kleffmann, J., and George, C.: Photosensitized reduction of nitrogen dioxide on humic acid as a source of nitrous acid, Nature, 440, 195, 10.1038/nature04603, 2006.

Takenaka, N., Soda, H., Sato, K., Terada, H., Suzue, T., Bandow, H., and Maeda, Y.: Difference in Amounts and Composition of Dew from Different Types of Dew Collectors, Water, Air, Soil Pollut., 147, 51-60, 10.1023/a:1024573405792, 2003.

VandenBoer, T. C., Brown, S. S., Murphy, J. G., Keene, W. C., Young, C. J., Pszenny, A. A. P., Kim, S., Warneke, C., de Gouw, J. A., Maben, J. R., Wagner, N. L., Riedel, T. P., Thornton, J. A., Wolfe, D. E., Dubé, W. P., Öztürk, F., Brock, C. A., Grossberg, N., Lefer, B., Lerner, B., Middlebrook, A. M., and Roberts, J. M.: Understanding the role of the ground surface in HONO vertical structure: High resolution vertical profiles during NACHTT-11, J. Geophys. Res. Atmos., 118, 10,155-110,171, doi:10.1002/jgrd.50721, 2013.

Vuollekoski, H., Vogt, M., Sinclair, V. A., Duplissy, J., Järvinen, H., Kyrö, E. M., Makkonen, R., Petäjä, T., Prisle, N. L., Räisänen, P., Sipilä, M., Ylhäisi, J., and Kulmala, M.: Estimates of global dew collection potential on artificial surfaces, Hydrol. Earth Syst. Sci., 19, 601-613, 10.5194/hess-19-601-2015, 2015.

Wang, G., Zhang, R., Gomez, M. E., Yang, L., Levy Zamora, M., Hu, M., Lin, Y., Peng, J., Guo, S., Meng, J., Li, J., Cheng, C., Hu, T., Ren, Y., Wang, Y., Gao, J., Cao, J., An, Z., Zhou, W., Li, G., Wang, J., Tian, P., Marrero-Ortiz, W., Secrest, J., Du, Z., Zheng, J., Shang, D., Zeng, L., Shao, M., Wang, W., Huang, Y., Wang, Y., Zhu, Y., Li, Y., Hu, J., Pan, B., Cai, L., Cheng, Y., Ji, Y., Zhang, F., Rosenfeld, D., Liss, P. S., Duce, R. A., Kolb, C. E., and Molina, M. J.: Persistent sulfate formation from London Fog to Chinese haze, Proceedings of the National Academy of Sciences, 113, 13630-13635, 10.1073/pnas.1616540113, 2016.

Wentworth, G. R., Murphy, J. G., Benedict, K. B., Bangs, E. J., and Collett Jr., J. L.: The role of dew as a night-time reservoir and morning source for atmospheric ammonia, Atmos. Chem. Phys., 16, 7435-7449, 10.5194/acp-16-7435-2016, 2016.

Wohlfahrt, G., Sapinsky, S., Tappeiner, U., and Cernusca, A.: Estimation of plant area index of grasslands from measurements of canopy radiation profiles, Agric. For. Meteorol., 109, 1-12, https://doi.org/10.1016/S0168-1923(01)00259-3, 2001.

Wong, K. W., Oh, H.-J., Lefer, B. L., Rappenglück, B., and Stutz, J.: Vertical profiles of nitrous acid in the nocturnal urban atmosphere of Houston, TX, Atmos. Chem. Phys., 11, 3595-3609, 10.5194/acp-11-3595-2011, 2011.

Ye, C., Gao, H., Zhang, N., and Zhou, X.: Photolysis of Nitric Acid and Nitrate on Natural and Artificial Surfaces, Environ. Sci. Technol., 50, 3530-3536, 10.1021/acs.est.5b05032, 2016.

Ye, Y., Zhou, K., Song, L., Jin, J., and Peng, S.: Dew amounts and its correlations with meteorological factors in urban landscapes of Guangzhou, China, Atmospheric Research, 86, 21-29, https://doi.org/10.1016/j.atmosres.2007.03.001, 2007.

Zhou, X., Gao, H., He, Y., Huang, G., Bertman, S. B., Civerolo, K., and Schwab, J.: Nitric acid photolysis on surfaces in low-NOx environments: Significant atmospheric implications, Geophys. Res. Lett., 30, 10.1029/2003gl018620, 2003.

Zhou, X., Zhang, N., TerAvest, M., Tang, D., Hou, J., Bertman, S., Alaghmand, M., Shepson, P. B., Carroll, M. A., Griffith, S., Dusanter, S., and Stevens, P. S.: Nitric acid photolysis on forest canopy surface as a source for tropospheric nitrous acid, Nature Geoscience, 4, 440-443, 10.1038/ngeo1164, 2011.

Role of the dew water on the ground surface in HONO distribution: a case measurement in Melpitz

Yangang Ren[1], Bastian Stieger[2], Gerald Spindler[2], Benoit Grosselin[1], Abdelwahid Mellouki[1*], Thomas Tuch[2], Alfred Wiedensohler[2], Hartmut Herrmann[2*],

1. Institut de Combustion, Aérothermique, Réactivité et Environnement (ICARE), CNRS (UPR 3021), Observatoire des Sciences de l'Univers en région Centre (OSUC), 1C Avenue de la Recherche Scientifique, 45071 Orléans Cedex 2, France

2. Leibniz Institute for Tropospheric Research (TROPOS), Permoserstraße 15, 04318 Leipzig, Germany

***** Corresponding author: Abdelwahid Mellouki (abdelwahid.mellouki@cnrs-orleans.fr) and Hartmut Herrmann (herrmann@tropos.de)

Abstract: To characterize the role of dew water for the ground/surface HONO distribution, nitrous acid (HONO) measurements with a MARGA and a LOPAP instrument were performed at the TROPOS research site in Melpitz from April 19th to 29th, 2018. The dew water was also collected and analyzed from May 8th to 14th, 2019 using a glass sampler. The high time resolution of HONO measurements showed characteristic diurnal variations that revealed: (i) vehicle emission is a minor source of HONO at the Melpitz station; (ii) heterogeneous conversion of NO_2 to HONO on ground surface dominates HONO production at night; (iii) there is significant nighttime loss of HONO with a sink strength of 0.16 ± 0.12 ppbv h^{-1}; (iv) dew water with mean NO_2^- of 7.91 ± 2.14 µg m^{-2} could serve as a temporary HONO source in the morning when the dew droplets evaporate. The nocturnal observations of HONO and NO_2 allowed direct evaluation of the ground uptake coefficients for these species at night: $\gamma_{NO2 \rightarrow HONO} = 2.4 \times 10^{-7}$ to 3.5×10^{-6}, $\gamma_{HONO,ground} = 1.7 \times 10^{-5}$ to 2.8×10^{-4}. A chemical model demonstrated that HONO deposition to the ground surface at night was 90-100% of the calculated unknown HONO source in the morning. These results suggest that dew water on the ground surface was controlling the temporal HONO distribution rather than straightforward NO_2–HONO conversion. This can strongly enhance the OH reactivity throughout morning time or other planted areas that provide large amount of ground surface based on the OH production rate calculation.

Keywords: HONO, ground surface, NO_2–HONO conversion, dew water, OH production

1 Introduction

Nitrous acid (HONO) is important in atmospheric chemistry as its photolysis (R1) is an important source of OH radicals. In the troposphere, OH radicals can initiate daytime photochemistry, not at least leading to the formation of ozone (O_3) and secondary organic aerosol (SOA).

$$HONO + h\nu \rightarrow OH + NO \quad (R1)$$

At present, the mechanisms of HONO formation have been and are still widely discussed. In the absence of light, heterogeneous reactions of NO_2 occur on wet surfaces (R2) and are considered to be an important source of HONO according to both laboratory studies and field observations (Acker et al., 2004).

$$2NO_2 + H_2O \rightarrow HONO + HNO_3 \quad (R2)$$

Finlayson-Pitts et al. (2003) proposed a mechanism (R3) involving the formation of the NO_2 dimer (N_2O_4) especially during nighttime. However, this pathway is not important in the real atmosphere (Gustafsson et al., 2008). The surface of soot (Ammann et al., 1998;Arens et al., 2001;Gerecke et al., 1998) or light activated soot (Aubin and Abbatt, 2007;Monge et al., 2010) contain functionalities attached to the large carbonaceous structures or individual condensed organic species, like phenol (R4) (Gutzwiller et al., 2002) and light-activated humic acids (Stemmler et al., 2006), which undergo electron transfer reactions with NO_2 yielding HONO (R5, where HA, A^{red}, and X are humic acid, activation of reductive centers and oxidants, respectively). This reaction is also postulated for aromatics in the aqueous phase, but only proceeds at a relevant rate at high pH levels (Ammann et al., 2005;Lahoutifard et al., 2002). Gustafsson et al. (2008) provide the evidence that formation of HONO proceeds by a bimolecular reaction of absorbed NO_2 and H (R6) on mineral dust, where H formed from the dissociation of chemisorbed water. However, Finlayson-Pitts (2009) indicated that this pathway is probably not transferable from laboratory to real atmosphere. In addition to the direct emission from the vehicle exhaust (Kurtenbach et al., 2001) and homogeneous gas phase reaction of NO with OH (R7) (Pagsberg et al., 1997), some other HONO formation mechanisms have been proposed e.g. homogeneous reaction of NO_2, H_2O, and NH_3 (R8) (Zhang and Tao, 2010); photolysis of nitric acid and nitrate (HNO_3/NO_3^-) (R9) (Ye et al., 2016;Zhou et al., 2011) and nitrite emission from soil (R10) (Su et al., 2011).

$$2NO_2\,(g) \leftrightarrow N_2O_4\,(g) \leftrightarrow N_2O_4\,(surface) \leftrightarrow HONO\,(surface) + HNO_3\,(surface) \quad (R3)$$

$$NO_2 + \{C\text{–}H\}_{red} \rightarrow HONO + \{C\}_{ox} \quad (R4)$$

$$HA \xrightarrow{h\nu} A^{red} + X;\ A^{red} + X \rightarrow A';\ A^{red} + NO_2 \rightarrow A'' + HONO \quad (R5)$$

$$NO_2\,(ads) + H\,(ads) \rightarrow HONO\,(ads) \rightarrow HONO\,(g) \quad (R6)$$

$$NO + OH \rightarrow HONO \quad (R7)$$

$$NO_2\,(g) + H_2O\,(g) + NH_3\,(g) \rightarrow HONO\,(g) + NH_4NO_3\,(s) \quad (R8)$$

$$HNO_3/NO_3^- + h\nu \rightarrow HONO/NO_2^- + O \quad (R9)$$

NO_2^- (aq) + H+ (aq) → HONO (aq) (R10)

Several studies (Acker et al., 2004;He et al., 2006;Lammel and Perner, 1988;Lammel and Cape, 1996;Rubio et al., 2009;VandenBoer et al., 2013;VandenBoer et al., 2014) reported that deposited HONO on wet surfaces can be a source for observed daytime HONO. He et al. (2006) observed HONO released from a drying forest canopy and their lab studies showed that, on average, ~90% of NO_2^- was emitted as HONO during dew evaporation. Rubio et al. (2009) found a positive correlation between formaldehyde and HONO in dew and the atmosphere.

The dominant loss of HONO is photolysis during daytime, which forms OH radicals (R1). An additional sink of HONO is the reaction with OH radical (R11). Due to the absence of solar radiation and the low OH concentration, the main loss process of HONO during nighttime is dry deposition, which can reach the balance with HONO production and vertical mixing to generate a steady state of HONO mixing ratio.

HONO + OH → H_2O + NO_2 (R11)

Due to its significant atmospheric importance, HONO has been measured for many years with various techniques (Febo et al., 1993;Huang et al., 2002;Kanda and Taira, 1990;Platt et al., 1980;Schiller et al., 2001;Wang and Zhang, 2000). LOng Path Absorption Photometer (LOPAP) is a two channel in situ HONO measurement instrument, which detects HONO continuously by wet sampling and photometric detection. LOPAP is very selective without sampling artefact and chemical interferences (e.g. NO_2, NO, O_3, HCHO, HNO_3, SO_2 and PAN etc.). In addition, the detection limit of LOPAP can go down to 0.2 pptv (Kleffmann and Wiesen, 2008) by optimizing the parameters like (a) sample gas flow rate, (b) liquid flow rates, and (c) the length of the absorption tubing (Heland et al., 2001). LOPAP was validated and compared with the most established and reliable HONO instrument Differential Optical Absorption Spectroscopy (DOAS) Both were used in the field and in a large simulation chamber under various conditions resulting in excellent agreement (Heland et al., 2001;Kleffmann et al., 2006).

The Monitor for AeRosols and Gases in ambient Air (MARGA) is a commercial instrument combining a Steam-Jet Aerosol Collector (SJAC) and a Wet Rotating Denuder (WRD), which can quantify the inorganic water-soluble PM ions (Cl^-, NO_3^-, SO_4^{2-}, NH_4^+, Na^+, K^+, Mg^{2+}, Ca^{2+}) and corresponding trace gases (HCl, HONO, HNO_3, SO_2, NH_3). In recent years, MARGA measurements were performed worldwide, which has been summarized by Stieger et al. (2018). Within the cited study HONO concentrations measured by a MARGA system and an off-line batch denuder without an inlet system were compared. Although the slope between both instruments was 1.10 with slightly higher MARGA concentrations in average, both instruments biased equally in the measured concentrations resulting in a high scattering with a coefficient of determination of $R^2 = 0.41$. The probable reason was the off-line analysis of the batch denuder sample as the resulting longer interaction of gas and liquid phase during the transport led to further heterogenous reactions. As both instruments

are based on the same sampling technique, the present study could be a good starting point for an inter-comparison between MARGA and LOPAP for HONO measurements to find possible reasons in the denuder deviations.

In this study, we present parallel measurements of HONO using LOPAP and MARGA in Melpitz, Germany, over two weeks in 2018. For further investigations, dew water was collected and analyzed from May 8th to 14th 2019 using two glass samplers. In addition, other water-soluble compounds, such as gaseous HNO_3, NH_3 and particulate NO_3^-, SO_4^{2-}, NH_4^+, Na^+, K^+, Mg^{2+}, Ca^{2+}, trace gases (NO_x, SO_2 and O_3) and meteorological parameters were also measured simultaneously. Our observations provide a direct inter-comparison between LOPAP and MARGA for HONO field measurement, additional insights into HONO chemical formation processes and examine the relative importance of dew as a sink and source of HONO.

2 Experimental

2.1 Site description

Measurements were performed at the research station of the Leibniz Institute for Tropospheric Research (TROPOS) in Melpitz (12°56′E, 51°32′N). This rural field site is situated on a meadow and surrounded by flat grass land, agricultural areas and forests. The Melpitz site mainly can be influenced by two different wind direction: west wind origin from the marine crossing a large area of Western Europe and the city of Leipzig (41 km NE), and east wind crossing Eastern Europe (Spindler et al., 2004).

2.2 MARGA instrument

The MARGA (1S ADI 2080, The Netherlands) used in this study has already been described in Stieger et al. (2018). Hence, only short information is provided here. An inlet flow of 1 m^3 hr^{-1} was drawn into the sampling box after passing through an inside Teflon-coated PM_{10} inlet (URG, Chapel Hill, 3.5 m). Within the sample box, the sampled air laminarly passed a WRD, in which water-soluble gases diffuse into a 10 mg l^{-1} hydrogen peroxide (H_2O_2) solution at pH = 5.7. Particles can reach the SJAC because of their smaller diffusion velocities. Within the SJAC, the particles grow into droplets under supersaturated water vapor conditions and were collected by a cyclone. The gas and particle samples are both collected over the course of one hour. Then, the aqueous samples of the WRD (gas phase) and the SJAC (particle phase) were successively injected into two ion-chromatographs (IC) with conductivity detectors (Metrohm, Switzerland) by two syringe pumps for analyzing the anions and cations. The volume of the injection loops for the anions and cations were 250 µl and 500 µl, respectively. The Metrosep A Supp 10 (75/4.0) column and Metrosep C4 (100/4.0) column were used to separate anions and cations, respectively. Lithium bromide was used as the internal standard for both gas- and particle-phase samples added during the sample injection to the IC.

The detection limits and the blanks for the MARGA system were performed before the intercomparison campaign in 2018. The detection limit of HONO was determined as 10 pptv. The blanks were analyzed when the system was set up in the field to consider potential contaminations. For blank measurements, the MARGA blank measurement mode was used that has a duration of six hours. Within the first 4 hours, the MARGA air pump was off and the denuder and SJAC liquids were analyzed. The first- and second-hour samples are discarded as they still include residual concentrations. The evaluation of the blank concentrations was performed for the third- and fourth-hour samples. No discernable peaks above the instrument detection limits were identified in both the gas and particle phase channels.

The precision for HONO quantification is below 4 % indicating a good repeatability. To test the robustness of the ion chromatography within the MARGA, standard solutions with defined NO_2^- concentrations of 70, 120 and 150 µg L^{-1} were injected in the IC system. The correlation between both the predefined concentrations within the standard solutions and the measured concentrations by the MARGA IC resulted in a slope of 1.13 (R^2 = 0.99). This value indicates slightly lower measured NO_2^- concentrations, which might be also a result of nonstable NO_2^- in freshly made liquid standard solutions.

2.3 LOPAP instrument

The LOPAP (QUMA, Germany) employed in this work was described in previous studies (Bernard et al., 2016;Heland et al., 2001). Only brief description is given here. The LOPAP instrument consists of two sections: a sampling unit and a detection unit. The ambient air was sampled in the sampling unit, which composed of two glass coils in series where the first coil (channel 1) accounted for HONO with interferences and the second coil (channel 2) sampled only interferences assuming that more than 99 % of HONO was absorbed into acidic stripping solution (pH=0) to form diazonium salt in channel 1. This salt reacts with a 0.8mM n-(1-naphthyl)ethylenediamine-dihydrochloride solution to produce final azo dye, which is photometrically detected by long path absorption in a special Teflon tubing (Heland et al., 2001;Kleffmann et al., 2006). During our field campaign in Melpitz, both the acidic stripping solution and 0.8mM n-(1-naphthyl)ethylenediamine-dihydrochloride solution were kept in the dark and were not changed during the whole campaign period. The temperature of the stripping coil was kept constant at 25 ℃ by a thermostat. Automatic zero air (Air liquid, Alphagaz 2, 99.9999%) measurements were performed for 30 min per 12 h measurements to correct for zero drifts. In addition, calibrations using NO_2^- standard solution (Heland et al., 2001) were applied in the beginning (April 17th), middle (April 20th, 24th, 25th) and end (April 29th) of the campaign to derive the HONO mixing ratio. The detection limit of LOPAP was approximately 1-2 pptv with a response time of 5 min. The error of HONO mixing ratio was estimated based on these detection limits and a relative error of 10%. The relative error is calculated by error propagation of all systematic errors, i.e. uncertainties in the gas flow ca. 2%, the liquid flow ca. 2 %, the error in the nitrite concentration during calibration 1 % and

errors for the used pipettes/flasks (two times of the specified errors of all volumetric glass ware since all glass ware was not used exactly at 20 ℃ like recommended by the manufacturer).

To investigate the possible sampling inlet and denuder artefacts of the MARGA, two different positions were selected for LOPAP during the measurement period (explained in SI): (M1) sampling unit of LOPAP was connected to the MARGA inlet in the back of the 2 m sampling tube and the PM_{10} inlet of MARGA as shown in Figure S1a (April 18th, 2018 13:00 UTC –April 20th, 2018 08:00 UTC); (M2) the sampling unit of LOPAP was settled in the same level as the sampling head of MARGA (Figure S1b) (April 20th, 2018 15:00 UTC –April 29th, 2018 07:00 UTC).

2.4 Dew water collection and analysis

To evaluate the HONO emission from the dew water in the morning, the dew water was collected one year later after the HONO comparison campaign and was analyzed on May 8th, 11th, 13th and 14th 2019. Similar conditions (grass height, dew formation and day length) were observed to improve the evaluation. For dew sampling, a glass sampler was used (as shown in Figure S2). Two 1.5 m^2 glass plates (Plate 1 and Plate 2) were placed 40 cm above the ground with a tilt angle of approximately 10 °. A gutter was installed at the lower end of each plates to collect the running down water. The water is trapped in 500 ml bottles. The dew samplers were prepared each evening before a likely dew event occurred (low dew point difference, clear sky and low winds). Each plate was rinsed with at least 2 L ultrapure water. A squeegee removed the excess water. Afterwards, the plates were cleaned with ethanol and were again rinsed by 2 L ultrapure water. The plate was splashed with ultrapure water and squeegeed six times and the gutter was cleaned. The sample of the sixth splash was collected as blank (~ 50 mL).

The dew water normally was collected from 18:00 to 5:00 (UTC). In the morning, the excess dew on the plate was squeegeed. To achieve the volume of dew (V_{dew}), the bottles were weighted before and after sampling by a balance. The pH was measured by a pH meter (mod. Lab 850, Schott Instruments) on a subsample of the total volume. After sampling, the aqueous solutions were filtered and stored in a fridge (~6 ℃). Within six hours, the HONO analyses of the dew and blank samples were performed by double-injection in the MARGA in the manual measurement mode as HONO may volatilize between sampling and analysis. For the other ions (Cl^-, NO_3^-, SO_4^{2-}, Oxalate, Br^- ,F^-, Formate, MSA , PO_4^{3-}, Na^+, NH_4^+, K^+ and Mg^{2+}, Ca^{2+}), the samples were analyzed with laboratory ion chromatogram systems (mod. ICS-3000, Dionex, USA). Blanks from water, the filter, the syringes and bottles were subtracted.

2.5 Aerosol measurements

The particle size distributions were measured in the size range from 5 nm to 10 μm employing by a Dual Mobility Particle Size Spectrometer (TROPOS-type D-MPSS) (Birmili

et al., 1999) and an Aerodynamic Particle Size Spectrometer (APSS model 3321, TSI Inc., Shoreview, MN, USA). For the particle number size distribution measurements, the aerosol is sampled through a low flow PM10 inlet and dried in an automatic diffusion dryer (Tuch et al., 2009). The measurements and quality assurance are done following the recommendations given in Wiedensohler et al. (2012) and Wiedensohler et al. (2018). The MPSS derived particle number size distribution was inverted by the algorithm described in Pfeifer et al. (2014), following the bipolar charge distribution of Wiedensohler (1988).

2.6 Other measurements

Trace gases of NO-NO_2-NO_x, SO_2 and O_3 were measured by NO_x analyzer (Thermo Model 42i-TL, Waltham, Massachusetts, USA), SO_2 analyzer APSA-360A and O_3 analyzer APOA 350 E (both Horiba, Kyoto, Japan) with a time resolution of 1 min. It should be noted that NO_2 was converted to NO within the NO_x analyzer by a blue light converter BLC2 (Meteorologie Consult GmbH, Königstein, Germany). The provider for replacement of the Mo-Converter in the 42i-TL analyzer is MLU Messtechnik GmbH, Essen Germany. Meteorological parameters like temperature (T), precipitation, relative humidity (RH) as well as wind velocity and direction were measured by PT1000, a rain gauge (R.M. Young Company, U.S.A.), the CS215 sensor (SensirionAG, Switzerland) and a WindSonic by Gill Instruments (UK), respectively. Global radiation and barometric pressure were recorded by a net radiometer CNR1 (Kipp&Zonen, The Netherlands) and a digital barometer (Vaisala, Germany), respectively.

2.7 Calculation of photolysis rate

Off-line NCAR Tropospheric Ultraviolet and Visible (TUV) transfer model (https://www2.acom.ucar.edu/modeling/tropospheric-ultraviolet-and-visible-tuv-radiation-model) was used to estimate the photolysis rate of HONO (J_{HONO}), NO_2 (J_{NO2}) and production rate of O^1D (J_{O1D}) at the Melpitz station scaled by the measured global radiation. Aerosol optical depth (AOD), total vertical ozone column, total NO_2 column, total cloud optical depth and surface reflectivity (Albedo) were taken from the NASA webpage for the period of measurement (https://neo.sci.gsfc.nasa.gov/blog/).

3 Results

3.1 Inter-comparison of LOPAP and MARGA

The hourly HONO mixing ratio obtained from MARGA with the 30 seconds and hourly averaged HONO mixing ratios from LOPAP are shown in Figure 1a and 1b, respectively. It indicates that the MARGA values were higher than the values of LOPAP. In addition, the comparison between both instruments in Figure 1a shows a delay of the MARGA concentrations after reaching the maximum concentrations in the morning. This pattern was

also observed in previous studies of Volten et al. (2012) and Dammers et al. (2017), who compared miniDOAS instruments with wet denuder systems. Compared to fast responses of the miniDOAS, the denuder-based instruments showed offsets and delays because of inlet memory artefacts by particles or water. Both groups also suggested transport effects of the liquid samples from the sampling to the analysis unit resulting in delays and slow responses.

The comparisons of the MARGA and LOPAP HONO measurements for period M1 and period M2 in Figure 1c result in slopes of 1.71 and 2.17 using error weighted Deming regression, respectively. This result is consistent with the former intercomparison of both instrument types in the Chinese field campaign (Lu et al., 2010;Xu et al., 2019) where the HONO mixing ratio measured with the wet-denuder-ion-chromatography (WD/IC) instrument was affected by a factor of three on average. Within the present work, we evaluated the relative importance of denuder artefact with the inlet artefact. The heterogeneous reactions of NO_2 with H_2O as well as NO_2 with SO_2 in water described by Spindler et al. (2003) or VOCs with NO_2 could explain the artefacts in the denuder solution (Kleffmann and Wiesen, 2008), which could account for ca. 71% (M1, where both LOPAP and MARGA used the common MARGA inlet) of these ca. 117% of overestimated HONO measurement from MARGA. Additional artefacts such as heterogeneous formation of HONO due to the long MARGA inlet system should be responsible for another ca. 46% (the difference between slopes M2 and M1). Hence, the results show that the use of massive sampling inlets, even if they are coated by Teflon, should be avoided for any in-situ HONO instrument. As a result, we chose the LOPAP-measured HONO in the following sections because of its high accuracy.

3.2 General results

Figure 2 and Figure 3 show an overview of the measured HONO, NO, NO_2, O_3, meteorological parameters, water-soluble ions in PM_{10} (NO_3^-, SO_4^{2-}, NH_4^+, Na^+, K^+, Mg^{2+}, Ca^{2+}) and their corresponding trace gases (HONO, HNO_3, SO_2, NH_3) in the present study. The daytime (D, 04:00-18:00, UTC) and nighttime (N, 18:00-04:00) averages are also provided in Table 1. During the two weeks measurement, the prevailing winds were from the southwest and northwest sectors, indicating a possible influence of city emission from Leipzig, Germany, on the site. The strong wind (maximum 13 m s^{-1}) led to low concentration of water-soluble ions in PM_{10} (NO_3^-, SO_4^{2-}, NH_4^+) and their corresponding trace gases (HNO_3, SO_2, NH_3) during the period April 24th to 29th, 2018. The air temperature ranged from 5 ℃ to 27 ℃ and the RH showed a clear variation pattern with higher levels during the night and lower levels during daytime. In addition, low mixing ratio of NO and NO_2 with a diurnal average of 0.9±1.2 ppbv and 3.7±2.2 ppbv, respectively, were recorded. These observations highlight the nature of our measurement site as a typical background environment. The HONO concentration from the LOPAP measurements varied from 30 pptv to 1582 pptv and showed diurnal variations (with average values of 162±96 pptv and 254±114 pptv during daytime and nighttime, respectively).

Größ et al. (2018) reported the linear function of the global radiation flux vs. OH radical concentration for the campaign EUCAARI 2008 at Melpitz.

$[OH]=A*Rad$ (Eq. 1)

with Rad being global solar irradiance in $W\,m^{-2}$ and [OH] is the hydroxyl radical concentration. The proportionality parameter A is 6110 $m^2\,W^{-1}\,cm^{-3}$. On the basis of such a correlation, we derived the OH concentration during the period of this field measurement, with an average of $(2.8\pm0.7)\times10^6$ during daytime.

3.3 Diurnal variation of HONO, particles and trace gas species

The diurnal profiles of HONO and related supporting parameters are shown in Figure 4 for the whole period except for two sets of observations: (1) no HONO peak in the morning of April 23rd and (2) HONO peak observed at 0:00-2:00 (UTC) of April 25th (Figure 5). Overall, the HONO increased fast after the sunrise and peaked at 7:00 (UTC), which then dropped rapidly and reached a minimum at around 10:00 (UTC) and kept until 17:00 (UTC). Such daytime pattern was also found in Spain, for a site surround by forests and sandy soils (Sörgel et al., 2011). Sörgel et al. (2011) explained this by local emissions, which are trapped in the stable boundary layer before its breakup of the inversion in the morning based on a similar diurnal cycle for NO and NO_2, which is different with this work. In this work, the NO_2 mixing ratio decreased from the midnight until noon and NO peaked at 5:00 (UTC) then kept low concentration (<1 ppbv) for 18 hours of one day. However, three hypotheses could be expected to explain this HONO morning peak: hypothesis (a) of HONO morning peak might possibly be caused by the photolysis of particle-phase HNO_3/NO_3^- (Ye et al., 2016;Zhou et al., 2003;Zhou et al., 2011), since as shown in Figure 4a, 4e and 4f, the early morning variation trend of HONO during daytime was similar to the one of NH_3 in the gas phase as well as NO_3^- and NH_4^+ in PM_{10}. Hypothesis (b), as reported by Stemmler et al. (2006), the photosensitized NO_2 on humic acid could act as a source of HONO during the daytime. For hypothesis (c), this morning peak of HONO has been reported for Melpitz (April 4th-14th, 2008) by Acker et al. (2004), who expected that the storage of HONO on wet surfaces can be a source for observed daytime HONO. Exactly, it was observed that dew was formed overnight during our campaign in Melpitz. Gaseous HONO could be deposited in these droplets. Due to evaporation after sunrise, HONO would be reemitted in the atmosphere and lead to a HONO morning peak. These hypotheses will be further discussed in Section 4.

As shown in Figure 4a and 4b, the HONO and NO_2 concentrations started to increase coincidentally at 16:00 (UTC) when the sunshine was weak. This could be explained by the variation of the vertical mixing increasing the level of all near ground emitted of formed species or by the heterogeneous conversion of NO_2 to HONO during nighttime and will be discussed in Section 4. The HONO mixing ratio then decreased from 21:00 (UTC) to around 100 pptv even though the NO_2 concentration kept constant around 5-6 ppbv. This decrease during nighttime indicates the HONO loss process (dry and wet deposition, trapped in the

boundary layer or dew etc.) surpassing the HONO formation from the NO_2-to-HONO conversion. The diurnal cycle of O_3 reflects the balance between the photochemical formation of O_3 (e.g. NO_2 + hv) and O_3 consumption (e.g. ozonolysis of terpenes).

3.4 HONO in the dew water

Dew water formation on canopy surfaces could be an efficient removal pathway of water soluble pollutants. High solubility of HONO makes dew water an efficient sink and a stable reservoir for atmospheric HONO. Actually, a lot of dew water has been observed on the grass around the Melpitz station during the sampling period of April 19th to 29th 2018. Hence, to investigate the dissolved HONO in the dew water of Melpitz station, the dew water was collected and analyzed from May 8th to 14th 2019 at the same season like the HONO measurements. Many ions e.g. NO_2^-, Cl^-, NO_3^-, SO_4^{2-}, Oxalate, Br^-, F^-, Formate, MSA, PO_4^{3-}, Na^+, NH_4^+, K^+ and Mg^{2+}, Ca^{2+} were analyzed using MARGA and laboratory IC, but our discussion only focuses on NO_2^-. The sample parameters (time, pH etc.) and NO_2^- concentration in the sample (µg L^{-1}) are shown in Table 2 from two glass plates (plate 1 and plate 2). The final dew water NO_2^- was calculated by subtracting the blank NO_2^- from the raw data of dew water analysis in MARGA. The pH of dew water in Melpitz ranged from 6.30 to 7.00. It should be noted that the dew water was frozen until 1 hour after sunrise on May 8th, 13th and 14th 2019 but not on May 11th 2019. At this day, a third sample was collected sampled from 3:30 to 5:20 (UTC) after collecting the first sample (18:00-3:20 UTC). The NO_2^- concentration per m^2 of the sampler surface (F_{NO2-}) was calculated from the following equation:

$$F_{NO2-} = \frac{[NO_2^-] \times V_{dew}}{S \times 1000} \quad \text{(Eq. 2)}$$

Where $[NO_2^-]$ is the sample concentration in µg L^{-1}, V_{dew} is the sample volume in ml, S is the surface area of the glass sampler as 1.5 m^2. As shown in Table 2, higher F_{NO2-} was obtained on May 11th where dew water was not frozen. On other days (May 8th, May 13th and May 14th) frozen dew water was observed, which likely inhibited HONO to dissolve. Hence, these frozen samples were not considered in this paper. On May 11th, the final F_{NO2}^- could be obtained by averaging F_{NO2}^- of the sum (9.43 µg m^{-2}) of the first and third sample with the second sample (6.40 µg m^{-2}) on 11th May resulting in mean 7.91±2.14 µg m^{-2}. This value will be used for the following calculation and discussion.

4 Discussion

4.1 Contribution of vehicle emissions

Because Melpitz site is close to a main national road from Leipzig to Torgau (Germany) that is within the main southwest wind direction, the contribution of vehicle emissions to the

measured HONO mixing ratio should be evaluated. Generally, the HONO/NO_x ratio is usually chosen to derive the emission factor of HONO in the freshly emitted plumes (Kurtenbach et al., 2001). As illustrated in Figure S3, NO_x concentrations were normally lower than 15 ppbv and NO/NO_x ratios were ~0.4 in this campaign, suggesting the detected air is a mixture of fresh and aged air during the measurement period. Therefore, a substantial part of HONO is secondary. Additionally, following the criteria of Li et al. (2018), the bad correlation between HONO and NO_x ($R^2 \approx 0.35$) suggests that the direct HONO emission from the vehicle emitted plumes were less important in this work.

4.2 Nighttime HONO

The nighttime HONO is different to some reported literatures (Huang et al., 2017;Li et al., 2012;Wang et al., 2017;Zhou et al., 2007). HONO increased after sunset to a maximum at 21:00 (UTC) and decreased until sunrise.

4.2.1 Formation through heterogeneous conversion of NO_2

The ratio of HONO/NO_2 is generally used as an index to estimate the efficiency of heterogeneous NO_2-HONO conversion because it is less influenced by transport processes than individual concentrations. However, the ratio might be influenced when a large fraction of HONO is emitted from the traffic but this is expected to be less important as shown in section 4.1. Then in this work, a low emission factor of 0.3% was used to correct the directly HONO emission from vehicles ($HONO_{corr}$) (Kurtenbach et al., 2001) . Six conditions as listed in Table 3 are selected to calculate the NO_2-HONO frequency following the criteria of Li et al. (2018):

(a) only the nighttime data in the absence of sunlight (i.e., 17:30-06:00 UTC) are used;
(b) both $HONO_{corr}$ and $HONO_{corr}$ / NO_2 ratios increased steadily during the target case;
(c) the meteorological conditions, especially surface winds, should be stable.

Figure S4 presents an example of the heterogeneous HONO formation occurring on April 28th, 2018. In this case, the HONO mixing ratios increased rapidly after sunset from 100 pptv to 600 pptv. Together with the HONO mixing ratio, the $HONO_{corr}/NO_2$ ratio increased almost linearly between 18:00 to 19:50 UTC. The slope fitted by the least squares regression for $HONO_{corr}/NO_2$ ratios against time can be taken as the conversion frequency of NO_2-to-HONO (k_{het}).

The ratio of $HONO_{corr}$ / NO_2 ranged from 0.055 to 0.161 with mean value of 0.110 ±0.041 (Table 3) using the data during early nighttime (17:30-00:00 UTC) in the Melpitz campaign. This mean values are within the wide range of reported values of 0.008-0.13 in the fresh air masses from the most sampling sites (Alicke et al., 2002;Alicke et al., 2003;Sörgel et al., 2011;Su et al., 2008;VandenBoer et al., 2013;Wang et al., 2017;Zhou et al., 2007) except for the study of Yu et al. (2009), who got a high value of 0.3. To our best knowledge, the present work presents also a high NO_2-to-HONO conversion frequency k_{het} of 0.027 ±0.017 h^{-1}

compared with most of the previous studies at urban sites, such as, Alicke et al. (2002) in Milan (0.012 h^{-1}), Wang et al. (2017) in Beijing (0.008 h^{-1}) and Acker and Möller (2007) in Rome (0.01 h^{-1}). However, our value is additionally comparable to Li et al. (2012) with 0.024 ± 0.015 h^{-1}, Alicke et al. (2003) with 0.018 ± 0.009 h^{-1} and Acker and Möller (2007) with 0.027 ± 0.012 h^{-1}, who also conducted rural measurements in the Pearl River Delta (PRD) area in Southern China, Pabstthum in Germany, and Melpitz, respectively, surrounded by farmland (grasses, trees, small forests). The higher value may suggest that a more efficient heterogeneous conversion from NO_2 to HONO is present in rural sites than in urban sites.

4.2.2 Relative importance of particle and ground surface in nocturnal HONO production

The particle surface density S_a was calculated as (0.4-9.9) $\times 10^{-4}$ m^2 m^{-3} from the particle size distribution (Figure S5a) ranged from 5 nm to 10 μm of APSS and D-MPSS data by assuming the particle are in spherical shape for the whole day period of April 19th-29th 2018. Due to the high RH (RH ~100% during nighttime in Figure S5b), the particle surface density S_a would be strongly enhanced (one magnitude) by the RH correction to be (0.5-1.9) $\times 10^{-3}$ m^2 m^{-3} with a hygroscopic factor $f(RH)$ following the method of Li et al. (2012) and Liu et al. (2008):

$$f(RH) = 1 + a \times (RH/100)^b \quad \text{(Eq. 3)}$$

where the empirical factors a and b were set to 2.06 and 3.6, respectively.

The formation of HONO through heterogeneous NO_2 conversion on particle surfaces (S_a) can be approximated following the recommendations in Li et al. (2010) by considering 100% HONO yield on the particle surface (NO_2+Org/soot/etc):

$$k_{het} = \frac{1}{4}\gamma_{NO2\rightarrow HONO\_a} \times \upsilon_{NO2} \times \frac{S_a}{V} \quad \text{(Eq. 4)}$$

where υ_{NO2} is the mean molecular velocity of NO_2 (370 m s^{-1}) (Ammann et al., 1998); S_a/V is the particle surface to volume ratio (m^{-1}) representing the surfaces available for heterogeneous reaction, and $\gamma_{NO2\rightarrow HONO\_a}$ is the uptake coefficient of NO_2 at the particle surface. Assuming the entire HONO formation was taking place on the particle surface, the calculated $\gamma_{NO2\rightarrow HONO\_a}$ from the Eq. 4 varied from 2.8×10^{-5} to 3.8×10^{-4} with a mean value of $(1.7 \pm 1.0) \times 10^{-4}$. This number is 2-3 orders of magnitude higher than typical uptake coefficients determined in the lab for the uptake of NO_2 in the dark on different substrates, e.g. Teflon/glass/NaCl/TiO_2/soot/Phenol etc: 10^{-6} to $<10^{-8}$ (Ammann et al., 1998;Gutzwiller et al., 2002;Kleffmann et al., 1998;Kurtenbach et al., 2001). Thus, this theoretical uptake coefficient clearly shows that formation on particles is not important. In addition, the weak correlations between $HONO_{corr}$ (R^2=0.566), $HONO_{corr}$/ NO_2 (R^2=0.208) and S_a (Figure S6) confirm that the HONO formed on particle surfaces could be unimportant as previously reported (Kalberer et al., 1999;Sörgel et al., 2011;Wong et al., 2011).

As illustrated above, the heterogeneous NO_2 conversion on ground surfaces (including surfaces such as plants, building, soils etc.) contributes mainly to nighttime formation of

HONO, which can be approximated by Eq. 5 following the method in literatures (Kurtenbach et al., 2001;Li et al., 2010;VandenBoer et al., 2013;VandenBoer et al., 2014) and also been applied by Zhang et al. (2016) by considering a 50% HONO yield from R2:

$$k_{het} = \frac{1}{8}\gamma_{NO2\rightarrow HONO\_g} \times \upsilon_{NO2} \times \frac{S_g}{V} \quad \text{(Eq. 5)}$$

where $\gamma_{NO2\rightarrow HONO\_g}$ is the uptake coefficient of NO_2 at the ground surface, S_g/V represents the ground surface to volume ratio. As described by Zhang et al. (2016), the LAI (m^2/m^2) was used to estimate the surface to volume ratio for the vegetation-covered areas, following the method in Sarwar et al. (2008):

$$\frac{S_g}{V} = \frac{2\times LAI}{H} \quad \text{(Eq. 6)}$$

Where H is the mixing layer height, which was calculated from the backward trajectory analysis based on GDAS data under dynamic conditions (Figure S7). The mixing layer height ranged between 20 m and 300 m from 17:00 until around 00:00 UTC in April 2018 (Figure S7). The LAI value is multiplied by a factor of 2 to take the areas on both sides of the leaves into account. In Wohlfahrt et al. (2001), the LAI for meadows with different grass heights are given. Regarding the grass height of ~30 cm in April 2018, we used a factor of 6 in present study. If the entire HONO formation was taking place on the ground surface, the calculated $\gamma_{NO2\rightarrow HONO\_g}$ varied from 2.4×10^{-7} to 3.5×10^{-6} with a mean value of $2.3\pm1.9\times10^{-6}$. This value agrees well with the reported range of $\gamma_{NO2\rightarrow HONO}$ from 10^{-6} to 10^{-5} on the ground surface based on the laboratory studies (Donaldson et al., 2014;VandenBoer et al., 2015) and field campaign in Colorado, USA (VandenBoer et al., 2013) during the night time. As the S/V ratio of particles is typically orders of magnitude lower than for ground surfaces, it is suggested that the heterogeneous reactions of NO_2 on the ground surface may play a dominant role for the nighttime HONO formation.

In addition, the relationship of NO_2-HONO conversion frequency (k_{het} presented in Table 3) with the inverse of wind speed is illustrated in Figure S8a. As indicated in Figure S8a, wind speed was predominantly less than 3 m s^{-1} during the field campaign period in Melpitz. High conversion frequency of NO_2-to-HONO mostly happened when wind speed was less than 1 m s^{-1}, which confirms that HONO formation mainly takes place on the ground. However, one point (in blue in Figure S8a) showed highest NO_2-HONO conversion frequency (k_{het}) when wind speed was ca. 4 m s^{-1} according to the second set of observation mentioned in section 3.3 and Figure 5. The likely reason for the temporary HONO peak is the dew droplet evaporation after increasing wind speed.

4.2.3 HONO deposition on the ground surface

As illustrated in Figure 4a and S4, between midnight and sunrise (19:00-4:00 UTC), the deposition of HONO becomes increasingly important as the absolute amount of HONO decreased. Assuming a constant conversion frequency of NO_2-to-HONO, k_{het}, the HONO

deposition rate (L_{HONO}) can be roughly estimated by:

$$L_{HONO} = \frac{d[HONO]}{dt} + k_{het} \times [NO_2] \quad \text{(Eq. 7)}$$

The strength of the HONO sink during night is in average 0.16±0.12 ppbv h^{-1} and ranged from 0.04 to 0.45 ppbv h^{-1}. This value is similar with reported ones in the literature (He et al., 2006).

The relationship of [HONO]/[NO_2] with RH during nighttime (18:00-04:00) is illustrated in Figure S8a. A positive trend of [HONO]/[NO_2] ratio along the RH was found when RH was less than 70%. However, [HONO]/[NO_2] performs a negative trend with RH for values over 70%. The same phenomenon was also observed by Yu et al. (2009) in Kathmandu and Li et al. (2012) in PRD region, China. This finding can be associated with larger amounts of water on various ground surfaces (plants and grasses) when ambient humidity approached saturation, leading to an efficient uptake of HONO.

Assuming all the extra HONO were removed through deposition on the ground surface, the change of HONO in the time interval of 22:00-04:00 (UTC) is parameterized using a combination of Eq. 7 and the following equation:

$$L_{HONO} = \frac{1}{4}\gamma_{HONO,ground} \times [HONO] \times \frac{\upsilon_{HONO}}{H} \quad \text{(Eq. 8)}$$

Where $\gamma_{HONO,ground}$ is the HONO uptake coefficient on the ground surface, υ_{HONO} is the mean molecular velocity of HONO with 3.67×10^4 cm s^{-1}, *H* is the mixing layer height calculated from the backward trajectory analysis ranging between 20 m and 150 m with an average of ca. 55 m from 22:00 until 04:00 UTC in April 2018. This approach yielded to a $\gamma_{HONO,ground}$ uptake coefficient in the range of 1.7×10^{-5} to 2.8×10^{-4} with an average of $(1.0\pm0.4)\times10^{-4}$, which is similar to data found in Boulder, Colorado, ranging from 2×10^{-5} to 2×10^{-4} (VandenBoer et al., 2013).

As observed by several studies (He et al., 2006;Rubio et al., 2009;Wentworth et al., 2016), the effective Henry's law solubility of HONO is highly pH-dependent (from borderline soluble at pH = 3 to highly soluble at pH ≥ 6), as would be expected for a weak acid. The pH of collected dew water during nighttime in May 2019 was 6.3-7.0 (Table 2), where the effective Henry's law solubility of HONO would be high. The amount of HONO in this dew water was quantified using MARGA and ranged between 42 and 165 µg L^{-1}, which is higher than NO_2^- in Santiago's dew waters (Rubio et al., 2009). This could strongly support the obtained HONO uptake coefficient on the ground surface. These field-derived surface parameters of nighttime HONO production from NO_2 and surface deposition of HONO are valuable to the model evaluation. However, it should be noted that the measured pH of collected dew from the glass plate might differ compared to the pH of dew found on soil or vegetated surfaces. The chemical nature of the material, with which the water is in contact, can influence the effective pH.

A simple resistance model based on the concept of aerodynamic transport, molecular diffusion

and uptake at the surface (presented in SI) as proposed by Huff and Abbatt (2002) was used to evaluate the factor(s) controlling the potential applicability of the γ-coefficients calculated here for the uptake of NO_2 and deposition of HONO. As shown in Figure S9, the deposition loss of HONO is potentially limited by a combination of aerodynamic transport, molecular diffusion and reaction processes. However, the HONO uptake will be transport-limited if the real uptake coefficients are ≥ 2.8×10^{-4} and wind speed was less than 0.5 m s^{-1}. In addition, molecular diffusion could play an important role for HONO uptake on the surface. Regarding the uptake of NO_2 on the ground surface, the range of NO_2 uptake coefficients as 2.4×10^{-7} to 3.5×10^{-6} obtained in the present work indicates limitation only by the reactive uptake process. The consistency between our findings and the values of these parameters in models (Wong et al., 2011;Zhang et al., 2016) suggests that the broad scale applicability of these field-derived terms for surface conversion of NO_2 should therefore be possible. However, those value of γ found for HONO ($\gamma_{HONO,\ ground}$=1.7×10^{-5} to 2.8×10^{-4}) require further exploration from various field environments and controlled lab studies.

4.3 Daytime HONO

HONO concentrations started to increase after sunrise and peaked at 7:00 (UTC) (Figure 4), during that time it also underwent photolysis, eventually reaching a steady state between 10:30–16:30 (UTC). Throughout the day, HONO was observed to reach an averaged minimum mixing ratio of 98 ±15 pptv. Since NO and NO_2 have not the same diurnal cycle as HONO (Figure 4), the R2 and R7 are not expected to be responsible for this HONO morning peak, but could contribute to the daytime HONO for the period of 10:30-16:30 (UTC).

4.3.1 Photostationary state in the gas phase

The measured diurnal daytime HONO could be compared to model results by assuming an instantaneous photo-equilibrium between the gas-phase formation (R7) and gas-phase loss processes (R1 and R11), which is described by the following expression (Kleffmann et al., 2005):

$$[\mathrm{HONO}]_{pss} = \frac{k_7[OH][NO]}{J_{HONO}+k_{11}[OH]} \quad \text{(Eq. 9)}$$

OH concentration was estimated from linear function of the global radiation flux vs. OH radical concentration as described in the previous section and shown in Figure 6, J_{HONO} was calculated using TUV model as described in section 2.6. The rate constants of NO+OH (k_7) and HONO+OH (k_{11}) used are 7.4×10^{-12} cm^3 $molecule^{-1}$ s^{-1} (Burkholder et al., 2015) and 6.0×10^{-12} cm^3 $molecule^{-1}$ s^{-1} (Atkinson et al., 2004), respectively. As a result, shown in Figure 6, the $[HONO]_{pss}$ (PSS, violet curve) could not explain the sudden HONO increase after sunrise but indicates a HONO peak around 4:40 (UTC) according to the relatively high NO concentration. However, some studies (Michoud et al., 2012;Sörgel et al., 2011) already discussed that the stationary state of HONO can be only reached during noontime. Hence, a

model calculation (named Model 1) was also used to discuss the HONO contribution from the gas-phase reaction of NO with OH radical.

$$\frac{d[HONO]}{dt} = k_7[OH][NO] + k_{het}[NO_2] - J_{HONO}[HONO] - k_{11}[HONO][OH] \quad \text{(Eq. 10)}$$

k_{het} derived from this work is 0.027 h^{-1}, [NO] and [NO_2] are averaged concentrations from field measurement. The results are shown in Figure 6 (orange line, Model 1). It is reasonable to indicate that the reaction of R7 only contribute 30-55% to the HONO increase in the early morning (4:30-7:30 UTC). R7 can continually contribute 50% of the measured HONO from 10:30 to 16:30 (UTC). However, regarding on the large uncertainty of [OH] (a factor of 2), the "unknown HONO sources" exist but could be not crucial. Basically, the additional HONO contribution rate could be estimated from the following equation:

$$P_{unknown} = \frac{d[HONO]}{dt} + J_{HONO}[HONO] + k_{11}[OH][HONO] - k_7[OH][NO] \quad \text{(Eq. 11)}$$

An additional source of 91 ±41 pptv h^{-1} was derived beside OH reaction with NO according to a HONO mixing ratio 98 ±15 pptv for the time period of 10:30 to 16:30 (UTC). This could be well explained by the photochemical processes such as R5 and R9 and would be discussed deeply in the next section.

4.3.2 Evidence for nighttime deposited HONO as a morning source

As observed in our field measurement and shown in Figure 2, the HONO concentrations always presented a strong increase from 4:00 – 7:00 (UTC), which induces three hypotheses as also mentioned in section 3.3: (a) photolysis of gas-phase and particulate nitrate, (b) photosensitized conversion of NO_2, (c) dew on ground surfaces served as HONO sink during the night and become a morning source by releasing the trapped nitrite back into ambient air.

To identify this HONO source, the chemical box model as expressed in Eq. 12 was extended with additional processes. Heterogeneous reaction of NO_2 on the wet surface (R2) and HONO deposition on the ground surface were firstly used to quantify the contributions of the well-known HONO production and loss processes. In addition, the HONO deposition on the ground surface independent on RH (24 hours, named Model 2) and with RH dependence (nighttime 17:00-8:00 UTC, named Model 3) are also discussed.

$$\frac{d[HONO]}{dt} = k_7[OH][NO] + k_{het}[NO_2] - J_{HONO}[HONO] - k_{11}[HONO][OH] - \frac{1}{4}\gamma_{HONO,ground}[HONO]\frac{\upsilon_{HONO}}{H} \quad \text{(Eq. 12)}$$

Both the surface production of HONO through NO_2 heterogeneous reaction and subsequent loss by ground surface deposition are already termed in Eq. 5 and Eq. 8, respectively. Here, k_{het} is 0.027 h^{-1} and $\gamma_{HONO,ground}$ is $(1.0 \pm 0.4) \times 10^{-4}$ calculated from the present observations. These values are applied to the model calculation to simulate the diurnal cycle of HONO. As shown in Figure 6, both Model 2 (blue line) and Model 3 (green square) cannot explain the HONO morning peak but Model 3 can well reproduce the nighttime HONO indicating that

surface loss of HONO is an important sink to consider when the RH was saturated. Hence, Model 3 was used as basic run for the following model calculation.

To investigate the contribution of photolysis of nitric acid and nitrate (HNO_3/NO_3^-) (R9) on the diurnal HONO based on the hypothesis (a), the following model calculation (Model 4, pink line) was made:

$$\frac{d[HONO]}{dt} = k_7[OH][NO] + k_{het}[NO_2] + J_{HNO3}[HNO_3/NO_3^-] - J_{HONO}[HONO] - k_{11}[HONO][OH] - \frac{1}{4}\gamma_{HONO,ground}[HONO]\frac{\upsilon_{HONO}}{H} \quad \text{(Eq. 13)}$$

Here gas-phase HNO_3 and particle NO_3^- are summed up and the photolysis frequency J_{HNO3} was derived from the TUV model by multiplying an enhanced factor of 30 due to a faster photolysis of particle-phase HNO_3 (Romer et al., 2018). As a result, the photolysis of HNO_3/NO_3^- (Model 4, pink line) could not reproduce the HONO morning peak shown in Figure 6. However, it could well reproduce the HONO for the time period of 10:30 to 16:30 (UTC).

To investigate the contribution of photosensitized conversion of NO_2 (R5) on the diurnal HONO based on the hypothesis (b), the following model calculation (Model 5) was performed:

$$\frac{d[HONO]}{dt} = k_7[OH][NO] + k_{het}[NO_2] + \frac{1}{4}(\gamma_a\frac{S_a}{V} + \gamma_g\frac{S_g}{V})\upsilon_{NO2}J_{NO2}[NO_2] - J_{HONO}[HONO] - k_{11}[HONO][OH] - \frac{1}{4}\gamma_{HONO,ground}[HONO]\frac{\upsilon_{HONO}}{H} \quad \text{(Eq. 14)}$$

Here the γ_a and γ_g are the light-enhanced NO_2 uptake coefficients both of 2.0×10^{-5} (Zhang et al., 2016) on both the aerosol surface and ground surface, respectively. J_{NO2} was multiplied with $\frac{light\ intensity}{400}$ when the light intensity is $\geq$ 400 W m^{-2}. As shown in Figure 6 (Model 5, cyan line), the photosensitized NO_2 on the aerosol and ground surface could not reproduce the HONO morning peak. This favors the third hypothesis that dew evaporation processes release HONO resulting in the sudden morning peak.

Indeed, as shown in Figure S10, the HONO morning peak always happens according to a fast decrease of RH between 4:30-9:00 (UTC). However, there is one case happened at 1:00 (UTC) on April 25th, 2018, possibly due to an upcoming strong wind which decreased the RH and evaporated the dew water on the ground surface. It should be noted that this HONO morning peak was never observed during this field measurement period without a fast RH decrease, in case of dry ground surface as it was observed during the morning of April 23rd, 2018. To figure out the relationship between temporary HONO emission from dew water and decreasing RH, the following equation was defined:

$$k_{emission} = \frac{d(\frac{HONO_{unknown}}{99.5-RH})}{dt} = \frac{\frac{HONO_{unknown}}{99.5-RH}(t_2) - \frac{HONO_{unknown}}{99.5-RH}(t_1)}{(t_2 - t_1)} \quad \text{(Eq. 15)}$$

where $HONO_{unknown} = HONO_{measure} - HONO_{Model4}$ was calculated for each day in the whole

campaign period. $k_{emission}$ could be obtained from the linear least square analysis of $\frac{HONO_{unknown}}{99.5-RH}$ vs. the internal time of HONO morning peak (4:30-7:00, UTC) as shown in Figure 7. The maximum and minimum of $k_{emission}$ are obtained as 0.026±0.008 and 0.006±0.001 pptv %$^{-1}$ s^{-1}, respectively, with an average of 0.016±0.014 pptv %$^{-1}$ s^{-1} as presented in Table 4. The average value was used in the following model calculation to reproduce the diurnal cycle of HONO.

$$\frac{d[HONO]}{dt} = k_7[OH][NO] + k_{het}[NO_2] + J_{HNO3}[HNO_3/NO_3^-] + \frac{1}{4}(\gamma_a\frac{S_a}{V} + \gamma_g\frac{S_g}{V})\upsilon_{NO2}J_{NO2}[NO_2] + k_{emission}*(99.5\text{-}RH) - J_{HONO}[HONO] - k_{11}[HONO][OH] - \frac{1}{4}\gamma_{HONO,ground}[HONO]\frac{\upsilon_{HONO}}{H} \quad \text{(Eq. 16)}$$

In Figure 6, the Model 6 (red line) shows that the amount of deposited HONO could represent the amount of HONO during the morning peak. In Figure S11, the measured atmospheric HONO mixing ratio and the calculated HONO mixing ratio using model 6 with a minimum dew HONO emission ($k_{emission}$ = 0.006 pptv %$^{-1}$ s^{-1}) and a maximum dew HONO emission ($k_{emission}$ = 0.026 pptv %$^{-1}$ s^{-1}) is shown. HONO emission from the dew water evaporation represented at least 90% and likely in excess of 100% of the calculated unknown HONO morning peak, which may continually serve as HONO source for the whole daytime as long as water evaporates depending on the weather condition.

4.3.3 HONO emission from dew water evaporation in the morning

The hypothetical morning HONO mixing ratio (pptv) due to the complete dew water evaporation could be estimated from the following equation by taking the measured dew nitrite and the mixing layer height:

$$[HONO] = \frac{\alpha \times S_g \times F_{NO2-}}{H \times S_g} = \frac{\alpha \times F_{NO2-}}{H} \quad \text{(Eq. 17)}$$

F_{NO2}^- is the NO_2^- concentration per m^2 of the glass sampler surface. The mean F_{NO2-} from May 11th 2019 was used for the calculation. S_g represents the surface area of the flat ground (analog to the surface area of the glass sampler), α is the enhanced factor for V_{dew} (dew water sample volume of the glass sampler in Eq.2) due to the larger cold surfaces from grass which can get in contact with humid air than the flat glass sampler. α was calculated as 2×LAI to take the areas on both sides of the leaves and the vegetation-covered areas on the ground into account. And a factor of 6 for LAI was assumed and used in section 4.2.2. However, regarding on the possibly different grass height during the HONO field measurement and dew measurements in April 2018 and May 2019, respectively, we would use a range of 1-6 for LAI in this section. During the HONO peak at 6 or 7 UTC, the mixing height ranged between 175 m and 600 m, while the value ranged from 20 m to 200 m at 0:00 – 5:00 UTC. Hence, the overall concentration increase from this source would be 377-2264, 189-1132, 76-122, 38-226 and 13-76 pptv, if all of the deposited HONO is released into the overlying air column for a

mixing height of 20, 40, 100, 200 and 600 m, respectively. Since the released HONO was subjected to photolysis, using a J_{HONO} from TUV model scaled by global radiation (section 2.7), a maximum [HONO] of 176-1053, 88-527, 35-211, 18-105 and 6-35 pptv for the mixing height 20, 40, 100, 200 and 600 m, respectively, would be contributed from the surface nitrite release at 7:00 UTC after the process started from 4:00 UTC. For a reasonable 100 m mixing height, this would account for 5-30% of the observed HONO morning peak in Figure 6. This low percentage might be a result of the different sampling time of dew measurement compared with HONO measurement and further studies are required for the exact quantification. Although the above calculations may be well simplified, the results do suggest that the release of the deposited HONO on wet/moist canopy surfaces may contribute to the morning HONO concentrations in the overlying atmosphere right after dew evaporation.

Indeed, few field studies (He et al., 2006;Rubio et al., 2009) have reported that dew water can serve as a sink and a temporary reservoir of atmospheric HONO. Previously, the role of dew as a nighttime reservoir and morning source for atmospheric NH_3 has been reported by Wentworth et al. (2016). Our results suggest that nocturnally deposited HONO forms a ground surface reservoir, which can be released in the following morning by dew evaporation. Therefore, a significant fraction of the daytime HONO source can be explained for the Melpitz observations.

4.3.4 Impact on the primary OH sources

HONO serves as an important primary source of OH during daytime in the troposphere (Kanaya et al., 2007;Kleffmann et al., 2005;Villena et al., 2011). Seiler et al. (2012) reported that the HONO is almost the only source of OH radicals in the early morning. The morning peak of HONO is mainly released from the dew evaporation and could imply a strong supply of OH radicals and, hence, enhances atmospheric oxidizing capacity in the atmosphere around Melpitz. Here, the net rate of OH radical from the HONO photolysis was calculated and compared with that from ozone photolysis, which is typically proposed as the major OH radical source in the atmosphere where water vapor is not limited.

$O_3 + h\nu \rightarrow O(^1D) + O_2$ (λ <320 nm) (R12)

$O(^1D) + H_2O \rightarrow 2OH$ (R13)

$O(^1D) + M \rightarrow O(^3P) + M$ (M =N_2) (R14)

Other OH sources, such as photolysis of oxidized VOCs, peroxides and ozonolysis of unsaturated VOCs are not considered due to the lack of measurement data for these radical precursors. The net rate of OH production from HONO photolysis ($P_{HONO->OH}$) was calculated by the source strength subtracting the sink terms due to reactions of R7 and R11. The OH production rate ($P_{O3->OH}$) from O_3 photolysis can be calculated by using the method proposed by Su et al. (2008) and Li et al. (2018).

$P_{HONO->OH} = J_{HONO}[HONO] - k_7[NO][OH] - k_{11}[HONO][OH]$ (Eq. 18)

$$P_{O3->OH} = 2J(O^1D)[O_3]\left(\frac{k_{13}[H_2O]}{k_{14}[M]+k_{13}[H_2O]}\right) \quad \text{(Eq. 19)}$$

Where $J(O^1D)$ was obtained from the TUV model scaled by the global radiation. The temperature dependence of k_{13} and k_{14} are taken from JPL/NASA Evaluation Number 18 (Burkholder et al., 2015). As shown in Figure 8, the photolysis of HONO produced similar amounts of OH compared with photolysis of ozone at the mean daytime (9:00-14:00, UTC), as $(7.2 \pm 2.0) \times 10^5$ molecule cm^{-3} s^{-1}. $P_{O3->OH}$ was, as expected, highest during the highest J values and negligible at the sunrise and sunset. $P_{HONO->OH}$ had a similar trend after the noontime but presented a strong OH production around 7:00 (UTC) due to the HONO morning peak. These results demonstrate the significant role of HONO in the atmospheric oxidizing capacity, especially for areas that experience frequent dew formation. In addition, the OH concentration calculated from the global radiation flux measurement was also shown in yellow color in Figure 8. The different trend of calculated OH concentration compared with P_{HONO} indicate that the morning OH concentration could be highly underestimated.

5 Conclusion and Atmospheric Implications

The inter-comparison of MARGA and LOPAP for the HONO measurement was applied from April 19th to 29th, 2018 at the Melpitz site. Higher HONO mixing ratio (ca. 117%) was obtained from MARGA compared with that of LOPAP caused by heterogeneous reactions within the MARGA WRD or potential sampling inlet artefact.

The maximum dew water NO_2^- concentration per m^2 of glass sampler surface was determined to be 7.91 ± 2.14 µg m^{-2}in May 2019. Thus, under consideration of photolytical losses and homogeneous mixing, the maximum contribution to the HONO morning peak from dew water evaporation could be calculated and ranged from 1053 ± 45 to 35 ± 1 pptv for mixing height of 20 to 600 m, respectively.

Well-defined diurnal cycles of HONO with concentration peaks in the early morning and in the evening are found. High time resolution of HONO measurements revealed (i) the vehicle emission is a negligible HONO source at the Melpitz site; (ii) HONO formed from the heterogeneous reaction NO_2 on the ground surface is the dominant nighttime source with a high NO_2-HONO conversion frequency of 0.027 ± 0.017 h^{-1}; (iii) significant amounts of HONO (0.16 ± 0.12 ppbv h^{-1}) deposited to the ground surface at night. The accurate observations of HONO and NO_2 allowed direct estimation of the ground uptake coefficients for these species at night: $\gamma_{NO2\rightarrow HONO\_g} = 2.4 \times 10^{-7}$ to 3.5×10^{-6}, $\gamma_{HONO,ground} = 1.7 \times 10^{-5}$ to 2.8×10^{-4}. The ground uptake coefficient of NO_2 and HONO are within the ranges of laboratory and model coefficients. The range of HONO uptake coefficient values calculated in this investigation are potentially limited by a combination of transport and diffusion to the ground surface.

A chemical model utilizing observational constraints on the HONO chemical system and known sources and sinks support the hypothesis that dew water on the ground surface,

especially on leaf surfaces, behave as a sink at night and a temporary reservoir for atmospheric HONO in the morning. The dew evaporation had a negative relationship with the RH in the atmosphere and, hence, the HONO emission rate was estimated to be 0.016 ± 0.014 pptv $\%^{-1}$ s^{-1} dependent on the RH after sunrise (start from 4:00, UTC). Furthermore, the formation and evaporation of dew on the ground surface influence significantly the air-surface exchange of HONO and, thus, its temporal distributions in the atmospheric boundary layer in the morning and night. The OH production rate from the photolysis of HONO compared with that from photolysis of O_3 showed that this dew emission of HONO can strongly enhance the OH reactivity throughout morning time and, hence, plays a vital role in the atmospheric oxidation.

Author contributions

RY wrote the paper with input from all authors. BS and GS analyzed the MARGA and dew data and wrote the paper. RY and BG conducted the HONO measurement using LOPAP. TT and AW were responsible for the particle measurement. AM and HH designed the experiments and lead the campaign. All co-authors commented on the manuscript.

Competing interests

The authors declare to have no competing interests.

Acknowledgements

The authors acknowledge financial support of this study and deployment of the MARGA system by the German Federal Environment Agency (UBA) research foundation under contracts No:351 01 093 and 351 01 070, as well as the European Union (EU) for the Transnational access (TNA) under ACTRIS-2: Comparison of HONO-measurements with MARGA and LOPAP at TROPOS research-site Melpitz (MARLO) is part of the project that has received funding from the European Union's Horizon 2020 research and innovation programme under grant agreement No 654109. For the laboratory analysis and the preparation of solutions, we thank A. Dietze, A. Rödger and S. Fuchs. For the support especially in the field, we thank R. Rabe and A. Grüner. We thank also the TROPOS mechanical workshop for the construction of the dew sampler. The CNRS team (Orléans-France) acknowledges the support from Labex Voltaire (ANR-10-LABX-100-01) and ARD PIVOTS program (supported by the Centre-Val de Loire regional council). Europe invests in Centre-Val de Loire with the European Regional Development Fund.

References

Acker, K., Spindler, G., and Brüggemann, E.: Nitrous and nitric acid measurements during the INTERCOMP2000 campaign in Melpitz, Atmos. Environ., 38, 6497-6505, 10.1016/j.atmosenv.2004.08.030, 2004.

Acker, K., and Möller, D.: Corrigendum to: Atmospheric variation of nitrous acid at different sites in Europe, Environ. Chem., 4, 364-364, https://doi.org/10.1071/EN07023_CO, 2007.

Alicke, B., Platt, U., and Stutz, J.: Impact of nitrous acid photolysis on the total hydroxyl radical budget during the Limitation of Oxidant Production/Pianura Padana Produzione di Ozono study in Milan, J. Geophys. Res. Atmos., 107, 8196, doi:10.1029/2000JD000075, 2002.

Alicke, B., Geyer, A., Hofzumahaus, A., Holland, F., Konrad, S., Pätz, H. W., Schäfer, J., Stutz, J., Volz-Thomas, A., and Platt, U.: OH formation by HONO photolysis during the BERLIOZ experiment, J. Geophys. Res. Atmos., 108, 8247, doi:10.1029/2001JD000579, 2003.

Ammann, M., Kalberer, M., Jost, D. T., Tobler, L., Rössler, E., Piguet, D., Gäggeler, H. W., and Baltensperger, U.: Heterogeneous production of nitrous acid on soot in polluted air masses, Nature, 395, 157, 10.1038/25965, 1998.

Ammann, M., Rössler, E., Strekowski, R., and George, C.: Nitrogen dioxide multiphase chemistry: Uptake kinetics on aqueous solutions containing phenolic compounds, Phys. Chem. Chem. Phys., 7, 2513-2518, 10.1039/B501808K, 2005.

Arens, F., Gutzwiller, L., Baltensperger, U., Gäggeler, H. W., and Ammann, M.: Heterogeneous Reaction of NO2 on Diesel Soot Particles, Environ. Sci. Technol., 35, 2191-2199, 10.1021/es000207s, 2001.

Atkinson, R., Baulch, D. L., Cox, R. A., Crowley, J. N., Hampson, R. F., Hynes, R. G., Jenkin, M. E., Rossi, M. J., and Troe, J.: IUPAC Task Group on Atmospheric Chemical Kinetic Data Evaluation, Atmos. Chem. Phys., 4, 1461-1738, 2004.

Aubin, D. G., and Abbatt, J. P. D.: Interaction of NO_2 with Hydrocarbon Soot: Focus on HONO Yield, Surface Modification, and Mechanism, J. Phys. Chem. A, 111, 6263-6273, 10.1021/jp068884h, 2007.

Bernard, F., Cazaunau, M., Grosselin, B., Zhou, B., Zheng, J., Liang, P., Zhang, Y. J., Ye, X. N., Daële, V., Mu, Y. J., Zhang, R. Y., Chen, J. M., and Mellouki, A.: Measurements of nitrous acid (HONO) in urban area of Shanghai, China, Environmental Science and Pollution Research, 23, 5818-5829, 10.1007/s11356-015-5797-4, 2016.

Birmili, W., Stratmann, F., and Wiedensohler, A.: Design of a DMA-based size spectrometer for a large particle size range and stable operation, J Aerosol Sci, 30, 549-553, 10.1016/S0021-8502(98)00047-0, 1999.

Burkholder, J. B., P. Sander, S., Abbatt, J., Barker, J. R., Huie, R. E., Kolb, C. E., Kurylo, M. J., Orkin, V. L., Wilmouth, D. M., and Wine, P. H.: Chemical Kinetics and Photochemical

Data for Use in Atmospheric Studies, Evaluation No. 18, in, edited by: JPL Publication 15-10, J. P. L., Pasadena,, 2015.

Dammers, E., Schaap, M., Haaima, M., Palm, M., Kruit, R. J. W., Volten, H., Hensen, A., Swart, D., and Erisman, J. W.: Measuring atmospheric ammonia with remote sensing campaign: Part 1-Characterisation of vertical ammonia concentration profile in the centre of The Netherlands, Atmos. Environ., 169, 97-112, 10.1016/j.atmosenv.2017.08.067, 2017.

Donaldson, M. A., Berke, A. E., and Raff, J. D.: Uptake of Gas Phase Nitrous Acid onto Boundary Layer Soil Surfaces, Environ. Sci. Technol., 48, 375-383, 10.1021/es404156a, 2014.

Febo, A., Perrino, C., and Cortiello, M.: A denuder technique for the measurement of nitrous acid in urban atmospheres, Atmos. Environ., 27, 1721-1728, 10.1016/0960-1686(93)90235-q, 1993.

Finlayson-Pitts, B. J., Wingen, L. M., Sumner, A. L., Syomin, D., and Ramazan, K. A.: The heterogeneous hydrolysis of NO_2 in laboratory systems and in outdoor and indoor atmospheres: An integrated mechanism, Phys. Chem. Chem. Phys., 5, 223-242, 10.1039/B208564J, 2003.

Finlayson-Pitts, B. J.: Reactions at surfaces in the atmosphere: integration of experiments and theory as necessary (but not necessarily sufficient) for predicting the physical chemistry of aerosols, Phys. Chem. Chem. Phys., 11, 7760-7779, 10.1039/b906540g, 2009.

Gerecke, A., Thielmann, A., Gutzwiller, L., and Rossi, M. J.: The chemical kinetics of HONO formation resulting from heterogeneous interaction of NO2 with flame soot, Geophysical Research Letters, 25, 2453-2456, 10.1029/98gl01796, 1998.

Größ, J., Hamed, A., Sonntag, A., Spindler, G., Manninen, H. E., Nieminen, T., Kulmala, M., Hõrrak, U., Plass-Dülmer, C., Wiedensohler, A., and Birmili, W.: Atmospheric new particle formation at the research station Melpitz, Germany: connection with gaseous precursors and meteorological parameters, Atmos. Chem. Phys., 18, 1835-1861, 10.5194/acp-18-1835-2018, 2018.

Gustafsson, R. J., Kyriakou, G., and Lambert, R. M.: The molecular mechanism of tropospheric nitrous acid production on mineral dust surfaces, ChemPhysChem, 9, 1390-1393, 10.1002/cphc.200800259, 2008.

Gutzwiller, L., Arens, F., Baltensperger, U., Gäggeler, H. W., and Ammann, M.: Significance of Semivolatile Diesel Exhaust Organics for Secondary HONO Formation, Environ. Sci. Technol., 36, 677-682, 10.1021/es015673b, 2002.

He, Y., Zhou, X., Hou, J., Gao, H., and Bertman, S. B.: Importance of dew in controlling the air-surface exchange of HONO in rural forested environments, Geophys. Res. Lett., 33, doi:10.1029/2005GL024348, 2006.

Heland, J., Kleffmann, J., Kurtenbach, R., and Wiesen, P.: A New Instrument To Measure Gaseous Nitrous Acid (HONO) in the Atmosphere, Environ. Sci. Technol., 35, 3207-3212, 10.1021/es000303t, 2001.

Huang, G., Zhou, X. L., Deng, G. H., Qiao, H. C., and Civerolo, K.: Measurements of atmospheric nitrous acid and nitric acid, Atmos. Environ., 36, 2225-2235, 10.1016/s1352-2310(02)00170-x, 2002.

Huang, R. J., Yang, L., Cao, J. J., Wang, Q. Y., Tie, X. X., Ho, K. F., Shen, Z. X., Zhang, R. J., Li, G. H., Zhu, C. S., Zhang, N. N., Dai, W. T., Zhou, J. M., Liu, S. X., Chen, Y., Chen, J., and O'Dowd, C. D.: Concentration and sources of atmospheric nitrous acid (HONO) at an urban site in Western China, Sci. Total Environ., 593, 165-172, 10.1016/j.scitotenv.2017.02.166, 2017.

Huff, A. K., and Abbatt, J. P. D.: Kinetics and Product Yields in the Heterogeneous Reactions of HOBr with Ice Surfaces Containing NaBr and NaCl, J. Phys. Chem. A, 106, 5279-5287, 10.1021/jp014296m, 2002.

Kalberer, M., Ammann, M., Arens, F., Gäggeler, H. W., and Baltensperger, U.: Heterogeneous formation of nitrous acid (HONO) on soot aerosol particles, J. Geophys. Res. Atmos., 104, 13825-13832, doi:10.1029/1999JD900141, 1999.

Kanaya, Y., Cao, R., Akimoto, H., Fukuda, M., Komazaki, Y., Yokouchi, Y., Koike, M., Tanimoto, H., Takegawa, N., and Kondo, Y.: Urban photochemistry in central Tokyo: 1. Observed and modeled OH and HO2 radical concentrations during the winter and summer of 2004, J. Geophys. Res. Atmos., 112, doi:10.1029/2007JD008670, 2007.

Kanda, Y., and Taira, M.: Chemiluminescent method for continuous monitoring of nitrous acid in ambient air, Anal. Chem., 62, 2084-2087, 10.1021/ac00218a007, 1990.

Kleffmann, J., Becker, K. H., and Wiesen, P.: Heterogeneous NO_2 conversion processes on acid surfaces: Possible atmospheric implications, Atmos. Environ., 32, 2721-2729, 10.1016/s1352-2310(98)00065-x, 1998.

Kleffmann, J., Gavriloaiei, T., Hofzumahaus, A., Holland, F., Koppmann, R., Rupp, L., Schlosser, E., Siese, M., and Wahner, A.: Daytime formation of nitrous acid: A major source of OH radicals in a forest, Geophys. Res. Lett., 32, doi:10.1029/2005GL022524, 2005.

Kleffmann, J., Lörzer, J. C., Wiesen, P., Kern, C., Trick, S., Volkamer, R., Rodenas, M., and Wirtz, K.: Intercomparison of the DOAS and LOPAP techniques for the detection of nitrous acid (HONO), Atmos. Environ., 40, 3640-3652, https://doi.org/10.1016/j.atmosenv.2006.03.027, 2006.

Kleffmann, J., and Wiesen, P.: Technical Note: Quantification of interferences of wet chemical HONO LOPAP measurements under simulated polar conditions, Atmos. Chem. Phys., 8, 6813-6822, 10.5194/acp-8-6813-2008, 2008.

Kurtenbach, R., Becker, K. H., Gomes, J. A. G., Kleffmann, J., Lörzer, J. C., Spittler, M., Wiesen, P., Ackermann, R., Geyer, A., and Platt, U.: Investigations of emissions and heterogeneous formation of HONO in a road traffic tunnel, Atmos. Environ., 35, 3385-3394, 10.1016/s1352-2310(01)00138-8, 2001.

Lahoutifard, N., Ammann, M., Gutzwiller, L., Ervens, B., and George, C.: The impact of multiphase reactions of NO_2 with aromatics: a modelling approach, Atmos. Chem. Phys., 2,

215-226, 10.5194/acp-2-215-2002, 2002.

Lammel, G., and Perner, D.: The atmospheric aerosol as a source of nitrous acid in the polluted atmosphere, J. Aerosol Sci., 19, 1199-1202, https://doi.org/10.1016/0021-8502(88)90135-8, 1988.

Lammel, G., and Cape, J. N.: Nitrous acid and nitrite in the atmosphere, Chem. Soc. Rev., 25, 361-369, 10.1039/CS9962500361, 1996.

Li, D., Xue, L., Wen, L., Wang, X., Chen, T., Mellouki, A., Chen, J., and Wang, W.: Characteristics and sources of nitrous acid in an urban atmosphere of northern China: Results from 1-yr continuous observations, Atmos. Environ., 182, 296-306, https://doi.org/10.1016/j.atmosenv.2018.03.033, 2018.

Li, G., Lei, W., Zavala, M., Volkamer, R., Dusanter, S., Stevens, P., and Molina, L. T.: Impacts of HONO sources on the photochemistry in Mexico City during the MCMA-2006/MILAGO Campaign, Atmos. Chem. Phys., 10, 6551-6567, 10.5194/acp-10-6551-2010, 2010.

Li, X., Brauers, T., Häseler, R., Bohn, B., Fuchs, H., Hofzumahaus, A., Holland, F., Lou, S., Lu, K. D., Rohrer, F., Hu, M., Zeng, L. M., Zhang, Y. H., Garland, R. M., Su, H., Nowak, A., Wiedensohler, A., Takegawa, N., Shao, M., and Wahner, A.: Exploring the atmospheric chemistry of nitrous acid (HONO) at a rural site in Southern China, Atmos. Chem. Phys., 12, 1497-1513, 10.5194/acp-12-1497-2012, 2012.

Liu, X., Cheng, Y., Zhang, Y., Jung, J., Sugimoto, N., Chang, S.-Y., Kim, Y. J., Fan, S., and Zeng, L.: Influences of relative humidity and particle chemical composition on aerosol scattering properties during the 2006 PRD campaign, Atmos. Environ., 42, 1525-1536, https://doi.org/10.1016/j.atmosenv.2007.10.077, 2008.

Lu, K., Zhang, Y., Su, H., Brauers, T., Chou, C. C., Hofzumahaus, A., Liu, S. C., Kita, K., Kondo, Y., Shao, M., Wahner, A., Wang, J., Wang, X., and Zhu, T.: Oxidant (O_3 + NO_2) production processes and formation regimes in Beijing, Journal of Geophysical Research: Atmospheres, 115, 10.1029/2009jd012714, 2010.

Michoud, V., Kukui, A., Camredon, M., Colomb, A., Borbon, A., Miet, K., Aumont, B., Beekmann, M., Durand-Jolibois, R., Perrier, S., Zapf, P., Siour, G., Ait-Helal, W., Locoge, N., Sauvage, S., Afif, C., Gros, V., Furger, M., Ancellet, G., and Doussin, J. F.: Radical budget analysis in a suburban European site during the MEGAPOLI summer field campaign, Atmos. Chem. Phys., 12, 11951-11974, 10.5194/acp-12-11951-2012, 2012.

Monge, M. E., D'Anna, B., Mazri, L., Giroir-Fendler, A., Ammann, M., Donaldson, D. J., and George, C.: Light changes the atmospheric reactivity of soot, Proceedings of the National Academy of Sciences, 107, 6605-6609, 10.1073/pnas.0908341107, 2010.

Pagsberg, P., Bjergbakke, E., Ratajczak, E., and Sillesen, A.: Kinetics of the gas phase reaction OH + NO(+M)→HONO(+M) and the determination of the UV absorption cross sections of HONO, Chem. Phys. Lett., 272, 383-390, https://doi.org/10.1016/S0009-2614(97)00576-9, 1997.

Pfeifer, S., Birmili, W., Schladitz, A., Müller, T., Nowak, A., and Wiedensohler, A.: A fast and

easy-to-implement inversion algorithm for mobility particle size spectrometers considering particle number size distribution information outside of the detection range, Atmos. Meas. Tech., 7, 95-105, 10.5194/amt-7-95-2014, 2014.

Platt, U., Perner, D., Harris, G. W., Winer, A. M., and Pitts, J. N.: Observations of nitrous acid in an urban atmosphere by differential optical absorption, Nature, 285, 312-314, 10.1038/285312a0, 1980.

Romer, P. S., Wooldridge, P. J., Crounse, J. D., Kim, M. J., Wennberg, P. O., Dibb, J. E., Scheuer, E., Blake, D. R., Meinardi, S., Brosius, A. L., Thames, A. B., Miller, D. O., Brune, W. H., Hall, S. R., Ryerson, T. B., and Cohen, R. C.: Constraints on Aerosol Nitrate Photolysis as a Potential Source of HONO and NOx, Environmental Science & Technology, 52, 13738-13746, 10.1021/acs.est.8b03861, 2018.

Rubio, M. A., Lissi, E., Villena, G., Elshorbany, Y. F., Kleffmann, J., Kurtenbach, R., and Wiesen, P.: Simultaneous measurements of formaldehyde and nitrous acid in dews and gas phase in the atmosphere of Santiago, Chile, Atmos. Environ., 43, 6106-6109, 10.1016/j.atmosenv.2009.09.017, 2009.

Sörgel, M., Regelin, E., Bozem, H., Diesch, J.-M., Drewnick, F., Fischer, H., Harder, H., Held, A., Hosaynali-Beygi, Z., Martinez, M., and Zetzsch, C.: Quantification of the unknown HONO daytime source and its relation to NO_2, Atmos. Chem. Phys., 11, 10433-10447, 10.5194/acp-11-10433-2011, 2011.

Sarwar, G., Roselle, S. J., Mathur, R., Appel, W., Dennis, R. L., and Vogel, B.: A comparison of CMAQ HONO predictions with observations from the Northeast Oxidant and Particle Study, Atmospheric Environment, 42, 5760-5770, https://doi.org/10.1016/j.atmosenv.2007.12.065, 2008.

Schiller, C. L., Locquiao, S., Johnson, T. J., and Harris, G. W.: Atmospheric measurements of HONO by tunable diode laser absorption spectroscopy, J. Atmos. Chem., 40, 275-293, 10.1023/a:1012264601306, 2001.

Seiler, W., Becker, K.-H., and Schaller, E.: Tropospheric Chemistry: Results of the German Tropospheric Chemistry Programme, Springer Netherlands, 2012.

Spindler, G., Hesper, J., Brüggemann, E., Dubois, R., Müller, T., and Herrmann, H.: Wet annular denuder measurements of nitrous acid: laboratory study of the artefact reaction of NO_2 with S(IV) in aqueous solution and comparison with field measurements, Atmos. Environ., 37, 2643-2662, 10.1016/s1352-2310(03)00209-7, 2003.

Spindler, G., Müller, T., Brüggemann, E., Gnauk, T., and Herrmann, H.: Long-term size-segregated characterization of PM_{10}, $PM_{2.5}$, and PM_1 at the IfT research station Melpitz downwind of Leipzig (Germany) using high and low-volume filter samplers, Atmos. Environ., 38, 5333-5347, 10.1016/j.atmosenv.2003.12.047, 2004.

Stemmler, K., Ammann, M., Donders, C., Kleffmann, J., and George, C.: Photosensitized reduction of nitrogen dioxide on humic acid as a source of nitrous acid, Nature, 440, 195, 10.1038/nature04603, 2006.

Stieger, B., Spindler, G., Fahlbusch, B., Müller, K., Grüner, A., Poulain, L., Thöni, L., Seitler, E., Wallasch, M., and Herrmann, H.: Measurements of PM_{10} ions and trace gases with the online system MARGA at the research station Melpitz in Germany – A five-year study, J. Atmos. Chem., 75, 33-70, 10.1007/s10874-017-9361-0, 2018.

Su, H., Cheng, Y. F., Shao, M., Gao, D. F., Yu, Z. Y., Zeng, L. M., Slanina, J., Zhang, Y. H., and Wiedensohler, A.: Nitrous acid (HONO) and its daytime sources at a rural site during the 2004 PRIDE-PRD experiment in China, J. Geophys. Res. Atmos., 113, doi:10.1029/2007JD009060, 2008.

Su, H., Cheng, Y. F., Oswald, R., Behrendt, T., Trebs, I., Meixner, F. X., Andreae, M. O., Cheng, P., Zhang, Y., and Poschl, U.: Soil Nitrite as a Source of Atmospheric HONO and OH Radicals, Science, 333, 1616-1618, 10.1126/science.1207687, 2011.

Tuch, T. M., Haudek, A., Müller, T., Nowak, A., Wex, H., and Wiedensohler, A.: Design and performance of an automatic regenerating adsorption aerosol dryer for continuous operation at monitoring sites, Atmos. Meas. Tech., 2, 417-422, 10.5194/amt-2-417-2009, 2009.

VandenBoer, T. C., Brown, S. S., Murphy, J. G., Keene, W. C., Young, C. J., Pszenny, A. A. P., Kim, S., Warneke, C., de Gouw, J. A., Maben, J. R., Wagner, N. L., Riedel, T. P., Thornton, J. A., Wolfe, D. E., Dubé, W. P., Öztürk, F., Brock, C. A., Grossberg, N., Lefer, B., Lerner, B., Middlebrook, A. M., and Roberts, J. M.: Understanding the role of the ground surface in HONO vertical structure: High resolution vertical profiles during NACHTT-11, J. Geophys. Res. Atmos., 118, 10,155-110,171, doi:10.1002/jgrd.50721, 2013.

VandenBoer, T. C., Markovic, M. Z., Sanders, J. E., Ren, X., Pusede, S. E., Browne, E. C., Cohen, R. C., Zhang, L., Thomas, J., Brune, W. H., and Murphy, J. G.: Evidence for a nitrous acid (HONO) reservoir at the ground surface in Bakersfield, CA, during CalNex 2010, Journal of Geophysical Research: Atmospheres, 119, 9093-9106, 10.1002/2013jd020971, 2014.

VandenBoer, T. C., Young, C. J., Talukdar, R. K., Markovic, M. Z., Brown, S. S., Roberts, J. M., and Murphy, J. G.: Nocturnal loss and daytime source of nitrous acid through reactive uptake and displacement, Nature Geoscience, 8, 55-60, 10.1038/ngeo2298, 2015.

Villena, G., Wiesen, P., Cantrell, C. A., Flocke, F., Fried, A., Hall, S. R., Hornbrook, R. S., Knapp, D., Kosciuch, E., Mauldin III, R. L., McGrath, J. A., Montzka, D., Richter, D., Ullmann, K., Walega, J., Weibring, P., Weinheimer, A., Staebler, R. M., Liao, J., Huey, L. G., and Kleffmann, J.: Nitrous acid (HONO) during polar spring in Barrow, Alaska: A net source of OH radicals?, Journal of Geophysical Research-Atmospheres, 116, 10.1029/2011jd016643, 2011.

Volten, H., Bergwerff, J. B., Haaima, M., Lolkema, D. E., Berkhout, A. J. C., van der Hoff, G. R., Potma, C. J. M., Kruit, R. J. W., van Pul, W. A. J., and Swart, D. P. J.: Two instruments based on differential optical absorption spectroscopy (DOAS) to measure accurate ammonia concentrations in the atmosphere, Atmos. Meas. Tech., 5, 413-427, 10.5194/amt-5-413-2012, 2012.

Wang, J., Zhang, X., Guo, J., Wang, Z., and Zhang, M.: Observation of nitrous acid (HONO) in Beijing, China: Seasonal variation, nocturnal formation and daytime budget, Sci. Total Environ., 587, 350-359, 10.1016/j.scitotenv.2017.02.159, 2017.

Wang, L. M., and Zhang, J. S.: Detection of nitrous acid by cavity ring down spectroscopy, Environ. Sci. Technol., 34, 4221-4227, 10.1021/es0011055, 2000.

Wentworth, G. R., Murphy, J. G., Benedict, K. B., Bangs, E. J., and Collett Jr., J. L.: The role of dew as a night-time reservoir and morning source for atmospheric ammonia, Atmos. Chem. Phys., 16, 7435-7449, 10.5194/acp-16-7435-2016, 2016.

Wiedensohler, A.: An approximation of the bipolar charge distribution for particles in the submicron size range, J. Aerosol Sci., 19, 387-389, https://doi.org/10.1016/0021-8502(88)90278-9, 1988.

Wiedensohler, A., Birmili, W., Nowak, A., Sonntag, A., Weinhold, K., Merkel, M., Wehner, B., Tuch, T., Pfeifer, S., Fiebig, M., Fjäraa, A. M., Asmi, E., Sellegri, K., Depuy, R., Venzac, H., Villani, P., Laj, P., Aalto, P., Ogren, J. A., Swietlicki, E., Williams, P., Roldin, P., Quincey, P., Hüglin, C., Fierz-Schmidhauser, R., Gysel, M., Weingartner, E., Riccobono, F., Santos, S., Grüning, C., Faloon, K., Beddows, D., Harrison, R., Monahan, C., Jennings, S. G., O'Dowd, C. D., Marinoni, A., Horn, H.-G., Keck, L., Jiang, J., Scheckman, J., McMurry, P. H., Deng, Z., Zhao, C. S., Moerman, M., Henzing, B., de Leeuw, G., Löschau, G., and Bastian, S.: Mobility particle size spectrometers: harmonization of technical standards and data structure to facilitate high quality long-term observations of atmospheric particle number size distributions, Atmos. Meas. Tech., 5, 657-685, 10.5194/amt-5-657-2012, 2012.

Wiedensohler, A., Wiesner, A., Weinhold, K., Birmili, W., Hermann, M., Merkel, M., Müller, T., Pfeifer, S., Schmidt, A., Tuch, T., Velarde, F., Quincey, P., Seeger, S., and Nowak, A.: Mobility particle size spectrometers: Calibration procedures and measurement uncertainties, Aerosol Sci. Technol., 52, 146-164, 10.1080/02786826.2017.1387229, 2018.

Wohlfahrt, G., Sapinsky, S., Tappeiner, U., and Cernusca, A.: Estimation of plant area index of grasslands from measurements of canopy radiation profiles, Agric. For. Meteorol., 109, 1-12, https://doi.org/10.1016/S0168-1923(01)00259-3, 2001.

Wong, K. W., Oh, H.-J., Lefer, B. L., Rappenglück, B., and Stutz, J.: Vertical profiles of nitrous acid in the nocturnal urban atmosphere of Houston, TX, Atmos. Chem. Phys., 11, 3595-3609, 10.5194/acp-11-3595-2011, 2011.

Xu, Z., Liu, Y., Nie, W., Sun, P., Chi, X., and Ding, A.: Evaluating the measurement interference of wet rotating-denuder–ion chromatography in measuring atmospheric HONO in a highly polluted area, Atmos. Meas. Tech., 12, 6737-6748, 10.5194/amt-12-6737-2019, 2019.

Ye, C., Gao, H., Zhang, N., and Zhou, X.: Photolysis of Nitric Acid and Nitrate on Natural and Artificial Surfaces, Environ. Sci. Technol., 50, 3530-3536, 10.1021/acs.est.5b05032, 2016.

Yu, Y., Galle, B., Panday, A., Hodson, E., Prinn, R., and Wang, S.: Observations of high rates

of NO_2-HONO conversion in the nocturnal atmospheric boundary layer in Kathmandu, Nepal, Atmos. Chem. Phys., 9, 6401-6415, 10.5194/acp-9-6401-2009, 2009.

Zhang, B., and Tao, F.-M.: Direct homogeneous nucleation of NO_2, H_2O, and NH_3 for the production of ammonium nitrate particles and HONO gas, Chem. Phys. Lett., 489, 143-147, 10.1016/j.cplett.2010.02.059, 2010.

Zhang, L., Wang, T., Zhang, Q., Zheng, J., Xu, Z., and Lv, M.: Potential sources of nitrous acid (HONO) and their impacts on ozone: A WRF-Chem study in a polluted subtropical region, J. Geophys. Res. Atmos., 121, 3645-3662, doi:10.1002/2015JD024468, 2016.

Zhou, X., Gao, H., He, Y., Huang, G., Bertman, S. B., Civerolo, K., and Schwab, J.: Nitric acid photolysis on surfaces in low-NOx environments: Significant atmospheric implications, Geophys. Res. Lett., 30, 10.1029/2003gl018620, 2003.

Zhou, X., Huang, G., Civerolo, K., Roychowdhury, U., and Demerjian, K. L.: Summertime observations of HONO, HCHO, and O_3 at the summit of Whiteface Mountain, New York, J. Geophys. Res. Atmos., 112, doi:10.1029/2006JD007256, 2007.

Zhou, X., Zhang, N., TerAvest, M., Tang, D., Hou, J., Bertman, S., Alaghmand, M., Shepson, P. B., Carroll, M. A., Griffith, S., Dusanter, S., and Stevens, P. S.: Nitric acid photolysis on forest canopy surface as a source for tropospheric nitrous acid, Nature Geoscience, 4, 440-443, 10.1038/ngeo1164, 2011.

Table 1. Mean and mean error as 2 times the standard deviation of the measured HONO (LOPAP) and the other pollutants in the Melpitz station during daytime (D, 04:00-18:00, UTC) and nighttime (N, 18:00-04:00, UTC).

	D	N		D	N
NO (ppbv)	1.0 ±0.5	0.5 ±0.3	HCl (ppbv) [b]	0.02 ±0.03	0.01 ±0.01
NOx (ppbv)	4 ±1	6 ±2	HNO_3 (ppbv) [b]	0.2 ±0.1	0.2 ±0.1
NO_2 (ppbv)	3 ±1	5 ±2	NH_3 (ppbv) [b]	17 ±7	8 ±4
HONO (pptv)[a]	162 ±96	254 ±114	Cl^- (μg m^{-3}) [b]	0.03 ±0.04	0.01 ±0.01
O_3 (ppbv)	36 ±7	19 ±13	NO_3^- (μg m^{-3}) [b]	3 ±2	2 ±1
SO_2 (ppbv)	0.8 ±0.4	0.5 ±0.3	SO_4^{2-} (μg m^{-3}) [b]	1.4 ±0.5	1.3 ±0.6
T (℃)	16 ±3	11 ±5	Na^+ (μg m^{-3}) [b]	0.02 ±0.03	0.01 ±0.01
RH (%)	67 ±7	85 ±11	NH_4^+ (μg m^{-3}) [b]	1.1 ±0.7	0.8 ±0.4
Wind speed (m s^{-1})	3 ±2	1.2 ±0.7	K^+ (μg m^{-3}) [b]	0	0.001 ±0.002
HONO/NOx (%)	0.04 ±0.02	0.05 ±0.02	Mg^{2+} (μg m^{-3}) [b]	0.03 ±0.01	0.02 ±0.04
NO/NOx (%)	0.3 ±0.1	0.1 ±0.1	Ca^{2+} (μg m^{-3}) [b]	0.2 ±0.1	0.2 ±0.1
OH (molecule cm^{-3})	(2.8 ±0.7) ×10^6		NO_2^- (μg m^{-3}) [b]	0.01 ±0.01	0.03 ±0.02

[a] HONO derived from LOPAP;

[b] data obtained from the MARGA instrument

Table 2. Nitrite concentration measured in dew water.

Date 2019	Plate number	Initial hour (UTC)	Final hour (UTC)	Volume (ml)	Blank NO_2^- ($\mu g\ L^{-1}$) [a]	Final NO_2^- ($\mu g\ L^{-1}$) [b]	F_{NO2-} ($\mu g\ m^{-2}$)	pH [c]
May 8th	1	18:00	5:25	76.60	0.0018	41.87	2.10	6.40
	2		5:45	75.60	0.0017	42.84	2.20	6.45
May 11th	1	18:00	3:20	94.00	0.0055	128.23	8.00	7.00
	2		4:20	80.00	0.0005	120.43	6.40	6.90
	1	3:30	5:20	13.00	0.0006	164.62	1.43	7.00
May 13th	1	18:00	4:45	72.00	0.0001	43.87	2.10	6.30
	2		5:20	79.00	0.0001	58.81	3.10	6.40
May 14th	1	18:00	5:00	15.00	0.0001	148.90	1.50	6.80
	2		5:00	21.00	0.0001	91.44	1.30	6.70

[a] note that the blank NO_2^- concentration is below the detection limit of 0.02 $\mu g\ L^{-1}$.

[b] Final NO_2^- = Raw NO_2^- - Blank NO_2^-

[c] pH was measured by a pH meter on a subsample of the total volume

Table 3. The ratio $HONO_{corr}/NO_2$ and the NO_2-HONO conversion frequency during early nighttime.

Date	UTC	R^2	$HONO_{corr}/NO_2$	k_{het} (h^{-1})
19/04/2018	17:30-19:50	0.45	0.118 ±0.010	0.043 ±0.002
21/04/2018	18:20-20:30	0.64	0.055 ±0.004	0.012 ±0.002
22/04/2018	18:10-21:20	0.79	0.161 ±0.005	0.030 ±0.002
25/04/2018	17:31-21:20	0.69	0.061 ±0.003	0.010 ±0.001
27/04/2018	18:00-23:41	0.48	0.113 ±0.006	0.016 ±0.001
28/04/2018	18:00-19:50	0.44	0.152 ±0.008	0.050 ±0.004
			0.110 ±0.041	0.027 ±0.017

Table 4. Summary of the temporary HONO emission rate from dew water, $k_{emission}$ from April 19th to 29th, 2018.

Period	$k_{emission}$ (pptv $\%^{-1}$ s^{-1})	
	Min	Max
21/4/2018	0.0054	0.0357
22/4/2018	0.0048	0.0314
24/4/2018	0.0057	0.0192
26/4/2018	0.0067	0.0302
27/4/2018	0.0048	0.0215
28/4/2018	0.0079	0.017
mean	0.006 ±0.001	0.026 ±0.008
Total average	0.016 ±0.014	

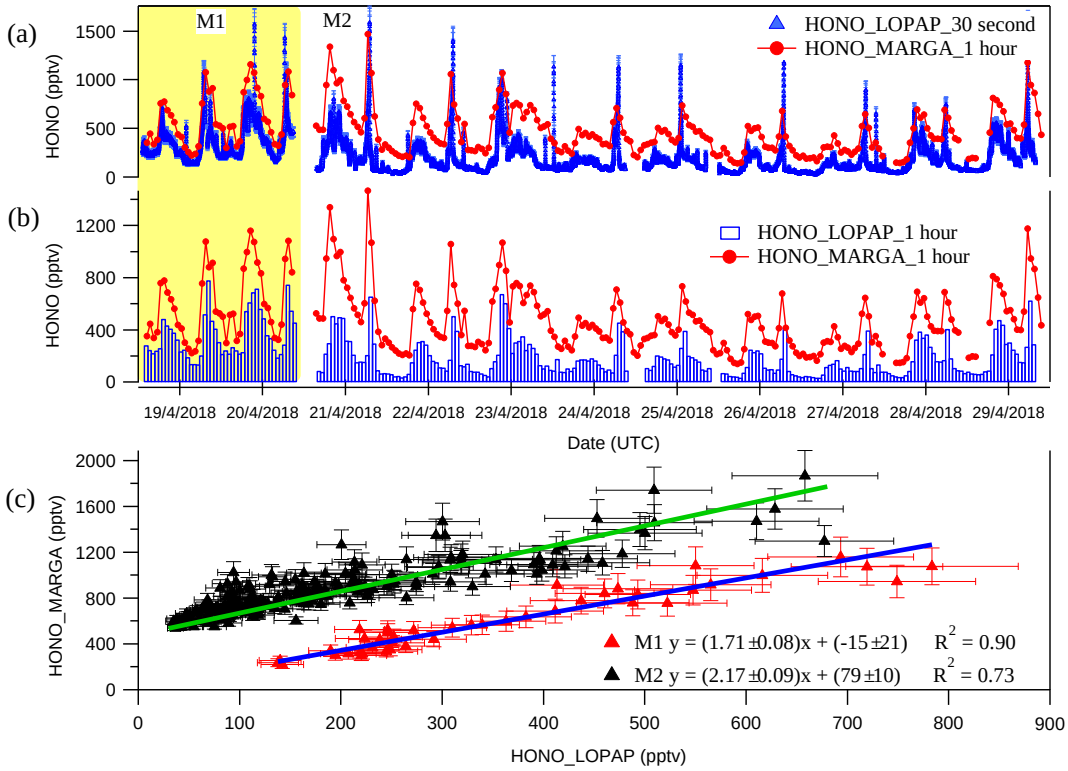

Figure 1. Time courses of HONO as hourly measured by MARGA and 30 seconds measured by LOPAP (a) and normalized hourly for LOPAP (b). (c) blue and green lines represent the error weighted orthogonal regression analysis between MARGA and LOPAP for two different comparison period of M1 and M2, respectively. The error bar in the panel (c) indicates the measurement error of HONO concentrations in LOPAP and MARGA. The HONO concentration of MARGA in panel (c) is shifted 400 pptv for clarity.

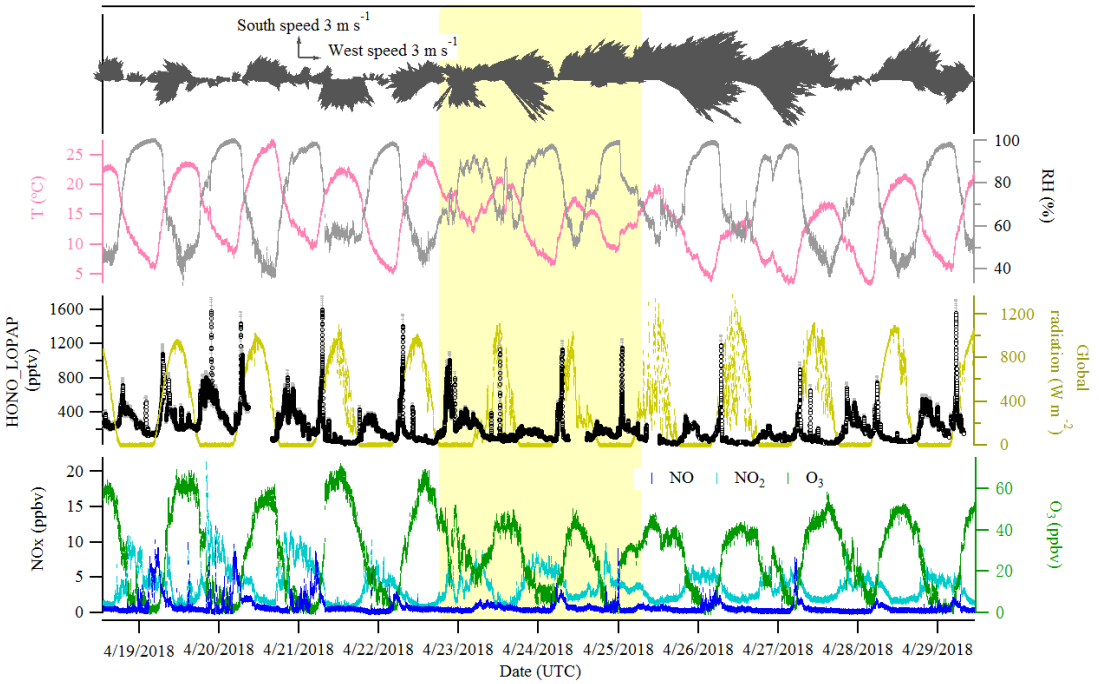

Figure 2. Time series of HONO (LOPAP measurement), NO, NO_2, O_3, global radiation, temperature (T), relative humidity (RH) and surface wind in Melpitz from April 19th to 29th, 2018. The gaps were mainly due to the maintenance of the instruments. The yellow shadow indicates two sets of observations discussed in section 3.3. The gray color in the HONO panel indicates the measurement error of HONO concentrations.

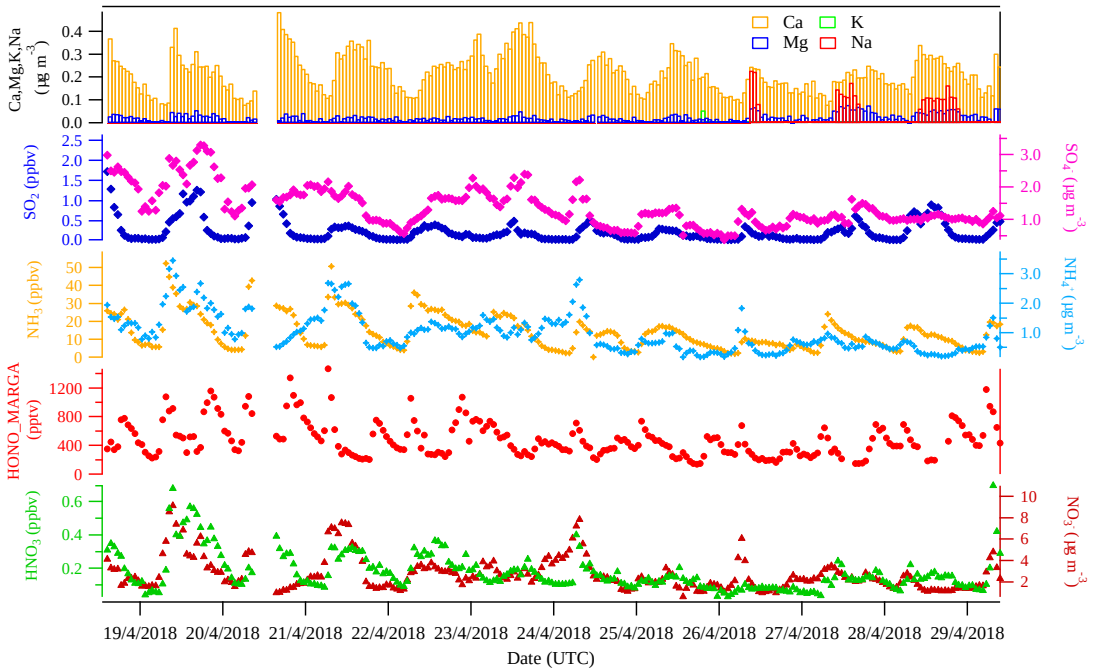

Figure 3. The hourly time-resolved quantification of water-soluble ions in PM_{10} (NO_3^-, SO_4^{2-}, NH_4^+, Na^+, K^+, Mg^{2+}, Ca^{2+}) and their corresponding trace gases (HONO, HNO_3, SO_2, NH_3) were measured by MARGA in Melpitz from April 19th to 29th, 2018.

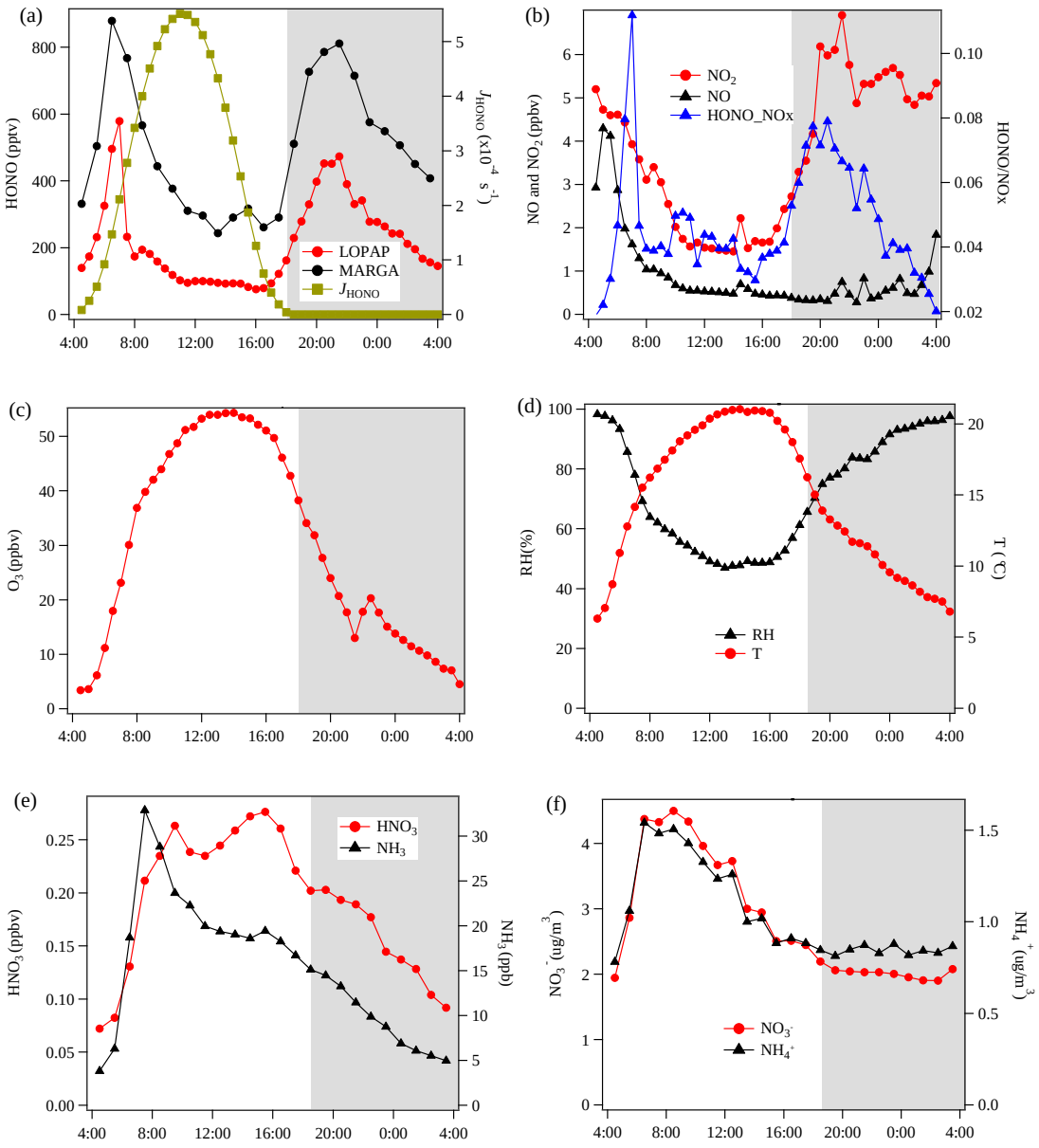

Figure 4. Diurnal variations of HONO and related species during the measurement period except for two sets of observations show in Figure 5 at Melpitz site. The photolysis rate of HONO was obtained from the TUV model. The grey shaded area indicates the nighttime period (18:00-04:00 UTC).

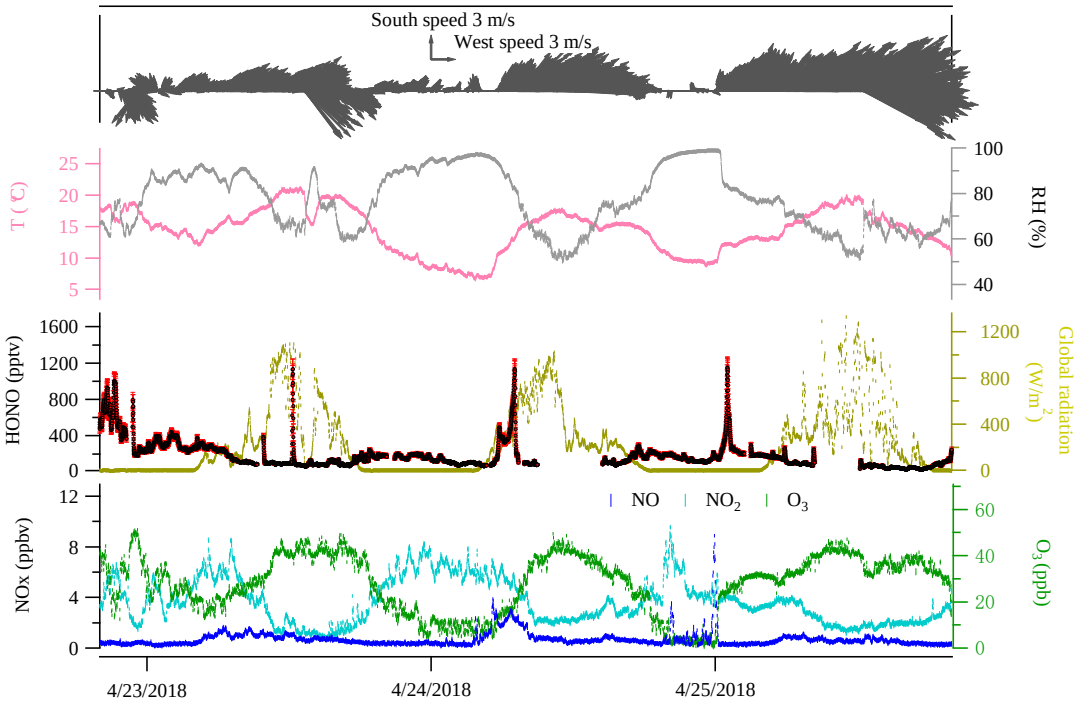

Figure 5. Case events for HONO (LOPAP) and related species at Melpitz site during the day April 23rd to 25th, 2018. The red color in the HONO panel indicates the measurement error of HONO concentrations.

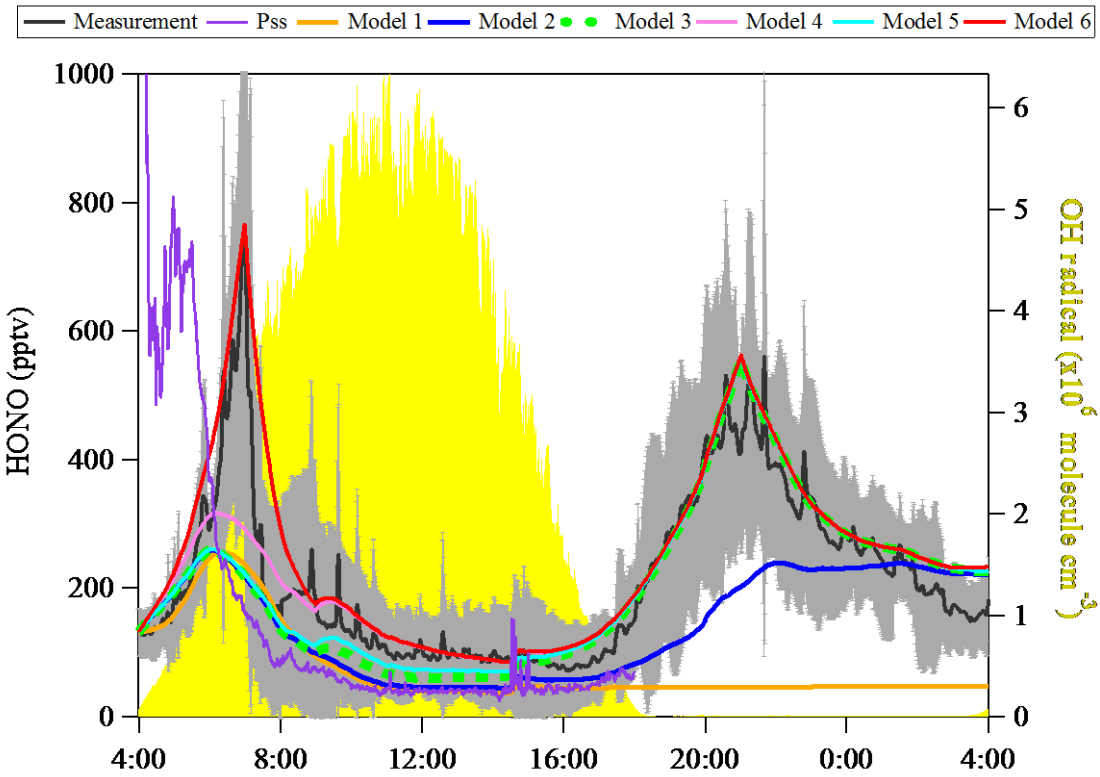

Figure 6. Observed average HONO atmospheric concentration (black line, +-1σ in shaded area) and the model calculated HONO concentration including different HONO production and loss processes. PSS presents model results by assuming an instantaneous photo-equilibrium between the gas-phase formation (R7) and gas-phase loss processes (R1 and R11) of HONO; Model 1 includes R1+R7+R11. Model 2 includes R1+R2+R7+R11+surface deposition (00:00-00:00), whereas Model 3 describes R1+R2+R7+R11+surface deposition (17:00-8:00). And Model 3 is used to be the base to investigate the effect of R9 (Model 4), R5 (Model 5) and the combination of R5+R9+Dew HONO emission (4:30-7:00) (Model 6).

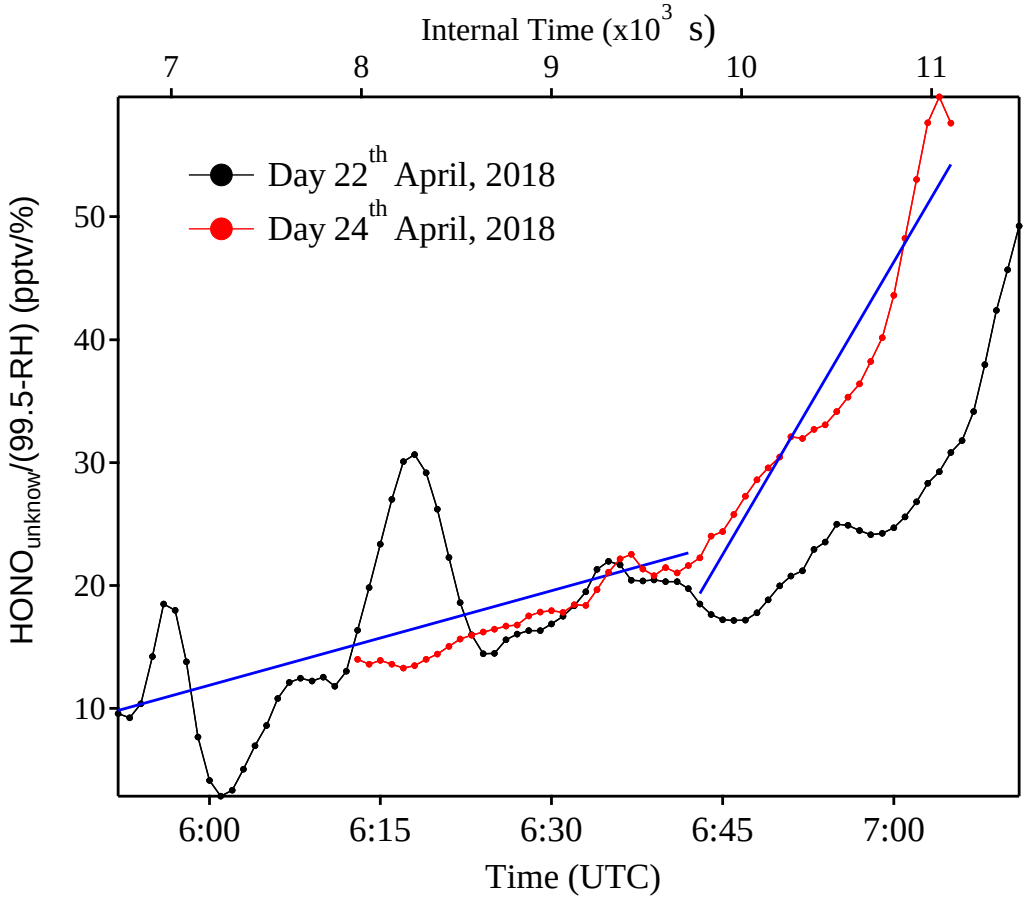

Figure 7. Example of $\frac{HONO_{unknown}}{99.5-RH}$ as a function of time (zero point from time 4:30, UTC) to estimate the temporary HONO emission rate from dew water ($k_{emission}$). Blue line is the linear least-square analysis of $\frac{HONO_{unknown}}{99.5-RH}$ vs. internal time to obtain the minimum (e.g. 22th April for the low slope) and maximum (e.g. 24th April for the high slope) of $k_{emission}$, respectively.

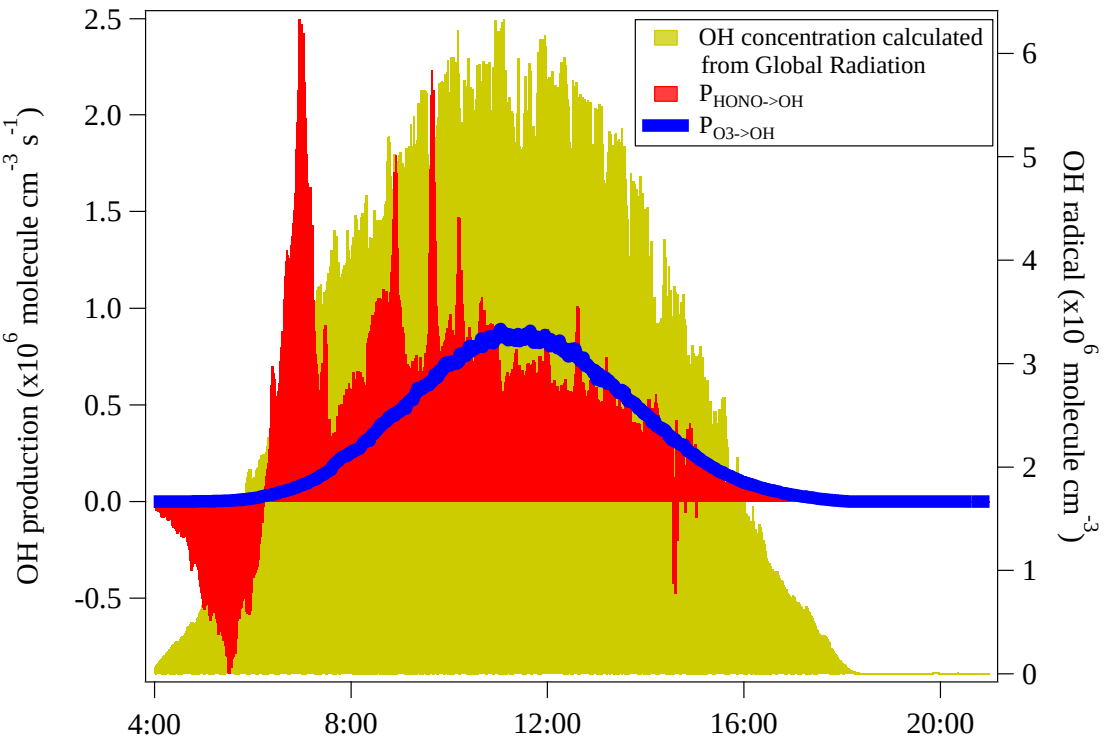

Figure 8. The OH production rates from photolysis of HONO and O_3 in Melpitz station from April 19th to 29th, 2018. The OH concentration is also shown as yellow area plot, which was calculated from the global radiation flux measurement: [OH]=A*Rad taken from Größ et al. (2018).